BRIEF REPORT

Serum (1→3) β-D-Glucan as a Noninvasive Adjunct Marker for the Diagnosis of *Pneumocystis* Pneumonia in Patients with AIDS

Tamayo Watanabe,[1,2] Akira Yasuoka,[3] Junko Tanuma,[1] Hirohisa Yazaki,[1,2] Haruhito Honda,[1] Kunihisa Tsukada,[1] Miwako Honda,[1] Hiroyuki Gatanaga,[1,2] Katsuji Teruya,[1] Yoshimi Kikuchi,[1] and Shinichi Oka[1,2]

[1]AIDS Clinical Center, International Medical Center of Japan, Tokyo, [2]Division of Infectious Disease, Center for AIDS Research, Kumamoto University, Kumamoto, and [3]Infection Control and Education Center, Nagasaki University, Nagasaki, Japan

High serum (1→3) β-D-glucan levels are described in patients with *Pneumocystis* pneumonia (PCP). We evaluated the diagnostic value of β-D-glucan in 111 patients with AIDS who had PCP and confirmed its usefulness. However, it does not correlate with disease severity and is not suitable for monitoring response to treatment.

Pneumocystis pneumonia (PCP) is associated with significant morbidity and mortality in patients with human immnuodeficiency virus type 1 (HIV-1) infection [1, 2]. PCP is usually diagnosed microscopically by identifying *Pneumocystis jirovecii* in bronchoalveolar lavage fluid (BALF) or bronchoscopically obtained lung tissue [3]. Bronchoscopy, however, is invasive, especially in patients with hypoxemia associated with PCP. Therefore, a minimally invasive method is desirable for diagnosis.

Serum (1→3) β-D-glucan (hereafter, β-D-glucan) is a common component of the cell wall of most fungi and is the major component of the cyst of *P. jirovecii*. Therefore, it is measured in patients who are suspected to have PCP, as well as in those with deep-seated mycotic infections [4]. Although β-D-glucan has been used as an adjunct test for the diagnosis of PCP [5], only a few reports have evaluated its level [5–7] and its correlation with other parameters (such as lactate dehydrogenase [LDH] level) in mixed populations that included a small number of HIV-infected patients [6]. For this purpose, we analyzed the correlation between β-D-glucan levels and other parameters among patients with AIDS who have PCP.

Methods. We evaluated data from 111 consecutive HIV-1–infected patients with PCP at the International Medical Center of Japan, an 885-bed tertiary care hospital in Tokyo, from April 1997 through July 2007. This study was approved by the Ethics Review Committee of the hospital (IMCJ-H20-569). Patients who did not undergo diagnostic bronchoscopy were excluded from the study.

Medical records were reviewed, and the following data were collected: age; sex; mode of infection; $CD4^+$ cell count; serum levels of LDH, β-D-glucan, and C-reactive protein (CRP); and alveolar-arterial oxygen tension gradient ($AaDO_2$). Serum β-D-glucan levels were measured using the Fungitec G MK test (Seikagaku). Manipulation was performed described elsewhere [4, 5], in accordance with the manufacturer's instructions. Serum β-D-glucan levels in HIV-1–infected patients without PCP determined during the same period were used as a control. If serum β-D-glucan levels had been determined several times for the same patient, only the first measurement was included. Although oral and esophageal candidiasis are superficial infections, they were included as an independent factor and analyzed. In this report, the term *candidiasis* refers to oral and/or esophageal candidiasis.

The diagnosis of PCP was established by identification of *P. jirovecii* in BALF. Each BALF specimen (100 μL) was centrifuged at 900 *g* for 2 min by means of a Shandon Cytospin III device, and a monolayer of deposited cells were stained using Diff-Quik (Dade Behring) and examined microscopically for the presence of *P. jirovecii*.

Data were expressed as means ± standard deviations (SDs) or as medians. Differences in categorical variables between patients with PCP and control patients were assessed using the Mann-Whitney *U* test. The Mann-Whitney *U* test (for comparison of 2 groups) and the Kruskal-Wallis test (for comparison of 3 groups) were used for analysis of differences in serum β-D-glucan levels. A receiver-operating-characteristic (ROC) curve was constructed to illustrate the cutoff value for β-D-glucan. The relationships were analyzed by linear regression analysis. Differences were considered significant at $P < .05$. Statistical analyses were performed using SPSS, version 17.0 (SPSS).

Results. A total of 111 patients had a definite diagnosis of PCP, and serum β-D-glucan level was measured in each. Of

Received 4 March 2009; accepted 27 May 2009; electronically published 2 September 2009.

Reprints or correspondence: Dr. Shinichi Oka, AIDS Clinical Center, International Medical Center of Japan, 1-21-1, Toyama, Shinjuku-ku, Tokyo 162-8655, Japan (oka@imcj.hosp.go.jp).

Clinical Infectious Diseases 2009; 49:1128–31

1058-4838/2009/4907-0024$15.00
DOI: 10.1086/605579

these patients, 67 also had candidiasis at admission. Of the control group (425 patients who did not have PCP), 28 had candidiasis, 3 had cryptococcal infection, and 394 had neither.

The patients with PCP were older than the control patients (mean ± SD, 42.3 ± 11.9 vs 38.7 ± 11.7 years; $P < .01$), and $CD4^+$ cell counts were significantly higher in the control patients than in the patients with PCP (mean ± SD, 178.6 ± 155.6 vs 49.1 ± 63.1 cells/μL; $P < .001$). Sex and mode of transmission of HIV were similar in both groups ($P = .81$ and $P = .53$, respectively). All patients with PCP received treatment, and 6 patients died of PCP.

Of the patients with PCP, 67 had candidiasis and 44 did not; of the control patients, 28 had candidiasis, 3 had cryptococcal infection, and 394 did not have any fungal infection. The median (range) serum β-D-glucan level in each group was 171.2 (14.9–2966), 209.6 (2.4–2469), 7.40 (1.0–73.0), 22.7 (9.3–69.7), and 8.25 (1.0–310) pg/mL, respectively (Figure 1). The median serum level of β-D-glucan among all patients with PCP (174.8 [2.4–2966] pg/mL) was significantly higher than that among the control patients (8.2 [1.0–310.1] pg/mL) ($P < .001$). The presence of candidiasis in both the PCP group and the control group and of cryptococcal infection in the control group did not significantly influence serum levels of β-D-glucan ($P = .53$, $P = .83$, and $P = .08$, respectively).

With respect to the diagnostic value of β-D-glucan, the area under the ROC curve for β-D-glucan level was 0.964 (95% confidence interval, 0.945–0.984) (Figure 2). A β-D-glucan cutoff value of 23.2 pg/mL (which represented the technique's threshold of detection) had a sensitivity of 96.4% and a specificity of 87.8%.

There was no correlation between serum levels of β-D-glucan and $AaDO_2$ at room air ($r = 0.125$; $P = .30$), LDH ($r = .030$; $P = .76$), or CRP ($r = .002$; $P = .62$). In 42 instances, serum β-D-glucan levels were measured before and after treatment. On the basis of a cutoff value of 23.2 pg/mL, normalization of serum β-D-glucan levels was noted in 7 patients. In contrast, serum β-D-glucan levels slightly increased in 9 patients despite clinical improvement being noted at week 3. This finding indicates that β-D-glucan levels reflected the clinical course in only 16.7% of patients (7 of 42) within 3 weeks of treatment.

Discussion. The present study has reported 3 major findings. The first major finding is the usefulness of quantitative measurement of serum β-D-glucan levels for the diagnosis of PCP. With a cutoff value of 23.2 pg/mL, β-D-glucan level had

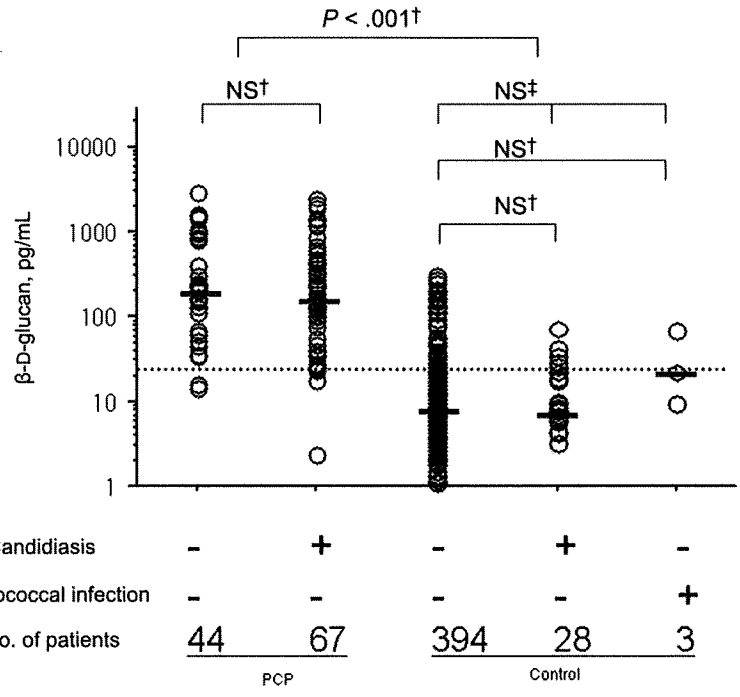

Figure 1. Serum levels of (1→3) β-D-glucan. Levels of β-D-glucan in serum were examined before treatment of *Pneumocystis* pneumonia (PCP), candidiasis, and cryptococcal infection. The Mann-Whitney *U* test (†) and the Kruskal-Wallis test (‡) were used for comparison of serum β-D-glucan levels. Individual values are plotted, and horizontal bars represents medians. The presence of candidiasis in both the PCP group and the control group and of cryptococcal infection in the control group did not significantly influence serum β-D-glucan levels ($P = .53$, $P = .83$, and $P = .08$, respectively). Serum β-D-glucan levels were significantly higher in patients with PCP than in those without PCP, despite the presence of candidiasis and cryptococcal infection ($P < .001$). NS, not significant.

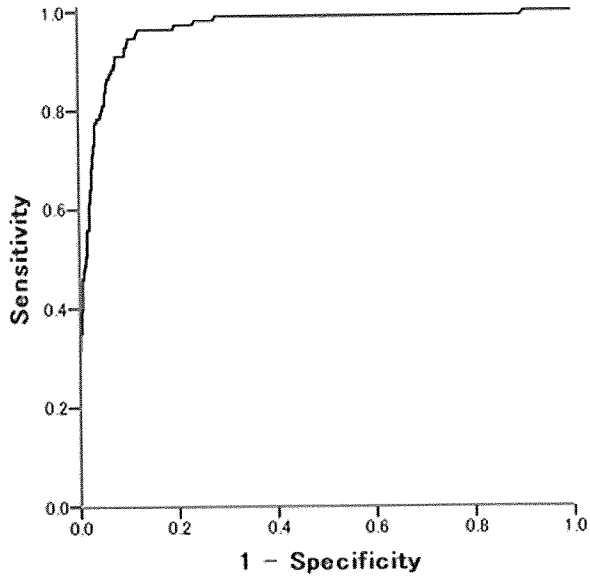

Figure 2. Receiver-operating-characteristic (ROC) curve for the (1→3) β-D-glucan cutoff. The area under the ROC curve for β-D-glucan was 0.964 (95% confidence interval, 0.945–0.984). A β-D-glucan cutoff value of 23.2 pg/mL (which represented the technique's threshold of detection) had a sensitivity of 96.4% and a specificity of 87.8%.

a high sensitivity (96.4%) and specificity (87.8%) for the diagnosis of PCP. Interestingly, serum β-D-glucan levels among those with PCP were not affected by the presence of superficial fungal infection (ie, oral and/or esophageal candidiasis). Deep-seated mycosis other than PCP and cryptococcal infection are quite rare in Japan, and no patients were suspected to have aspergillosis in this study. Hence, we could not analyze the effect of aspergillosis. According to our data and those of others [4], β-D-glucan level increases during cryptococcal infection, but the level is significantly lower than that observed during PCP. The number of *P. jirovecii* organisms in the lungs of patients with AIDS may be significantly higher than that in patients without AIDS [8]. In a meta-analysis of 7 reports in which PCP was diagnosed by staining, the average sensitivity of induced sputum was 56%, whereas that of BALF was >95% [9]. To eliminate false-positive and false-negative results, we analyzed data obtained only from patients who underwent BALF analysis and had a definite diagnosis of PCP.

The second major finding was that the serum level of β-D-glucan does not reflect the severity of PCP in patients with AIDS. Although Shimizu et al [10] reported that β-D-glucan is a negative prognostic marker for PCP in patients with connective tissue diseases, there was no significant difference in β-D-glucan level between survivors and nonsurvivors in our study. Furthermore, Tasaka et al [6] reported that serum levels of LDH correlated with those of β-D-glucan in patients with PCP, whereas our data showed no such relationship. These differences are probably the result of differences in the patient populations studied, especially regarding whether the patients have HIV-1 infection. Considered collectively, these results emphasize the need for further studies to define the exact relationship between β-D-glucan and prognosis as well as LDH.

The third major finding of the present study was that β-D-glucan level did not reflect the effectiveness of therapy. In nearly 85% patients, serum β-D-glucan levels did not decrease to normal despite clinical improvement. Furthermore, 20% of patients had increased levels of β-D-glucan during the early phase of treatment. However, β-D-glucan levels normalized several months or years after treatment in all patients. These results mean that β-D-glucan levels increase transiently early during treatment and decrease thereafter but do not always return to normal during treatment. The transient increase in β-D-glucan level is probably due to lysis of *P. jirovecii* shortly after treatment.

PCP is usually suspected on the basis of chest radiographic findings, clinical symptoms, and low $CD4^+$ cell counts in HIV-infected patients. In the present study, a high serum level of β-D-glucan (especially >23.2 pg/mL by the MK test) was found to be highly indicative of PCP in practically all patients with AIDS. Therefore, the β-D-glucan test is useful for the diagnosis of PCP, especially in HIV-infected patients who are unable to undergo bronchoscopy owing to severe hypoxemia. In conclusion, the present study has demonstrated that β-D-glucan is a useful, noninvasive adjunct marker for the diagnosis of PCP in patients with AIDS. However, its serum levels do not reflect the severity of the disease, and it is not suitable for monitoring response to treatment.

Acknowledgments

We thank all staff of the AIDS Clinical Center for the care of patients.

Financial support. Ministry of Health, Labour, and Welfare of Japan (grant for AIDS research AIDS-H18-008).

Potential conflicts of interest. All authors: no conflicts.

References

1. Kaplan JE, Hanson D, Dworkin MS, et al. Epidemiology of human immunodeficiency virus–associated opportunistic infections in the United States in the era of highly active antiretroviral therapy. Clin Infect Dis **2000**; 30(Suppl 1):S5–14.
2. Mocroft A, Katlama C, Johnson AM, et al. AIDS across Europe, 1994–98: the EuroSIDA study. Lancet **2000**; 356:291–6.
3. Cushion MT, Beck JM. Summary of *Pneumocystis* research presented at the 7th International Workshop on Opportunistic Protists. J Eukaryot Microbiol **2001**; 48(Suppl):101S–5S.
4. Obayashi T, Yoshida M, Mori T, et al. Plasma (1→3)-beta-D-glucan measurement in diagnosis of invasive deep mycosis and fungal febrile episodes. Lancet **1995**; 345:17–20.
5. Yasuoka A, Tachikawa N, Shimada K, Kimura S, Oka S. (1→3) beta-D-glucan as a quantitative serological marker for *Pneumocystis carinii* pneumonia. Clin Diagn Lab Immunol **1996**; 3:197–9.

6. Tasaka S, Hasegawa N, Kobayashi S, et al. Serum indicators for the diagnosis of pneumocystis pneumonia. Chest **2007**; 131:1173–80.
7. Marty FM, Koo S, Bryar J, Baden LR. (1→3) beta-D-glucan assay positivity in patients with *Pneumocystis (carinii) jiroveci* pneumonia. Ann Intern Med **2007**; 147:70–2.
8. Thomas CF Jr, Limper AH. *Pneumocystis pneumonia.* N Engl J Med **2004**; 350:2487–98.
9. Cruciani M, Marcati P, Malena M, Bosco O, Serpelloni G, Mengoli C. Meta-analysis of diagnostic procedures for *Pneumocystis carinii* pneumonia in HIV-1-infected patients. Eur Respir J **2002**; 20:982–9.
10. Shimizu A, Oka H, Matsuda T, Ozaki S. (1→3)-beta-D glucan is a diagnostic and negative prognostic marker for *Pneumocystis carinii* pneumonia in patients with connective tissue disease. Clin Exp Rheumatol **2005**; 23:678–80.

Raltegravir-associated perihepatitis and peritonitis: a single case report

Raltegravir, the first approved HIV integrase inhibitor, has demonstrated an excellent safety and tolerability profile in several clinical trials [1] and is currently used widely as one of the key components of salvage regimens. However, the duration of clinical use is relatively short, and unknown adverse effect may occur. Here, we report one case of peritonitis associated with use of raltegravir. Abdominal symptoms appeared within 2 weeks of commencement of treatment, and raltegravir had to be stopped due to worsening of clinical condition.

Case report

The patient was a 49-year-old Japanese hemophiliac coinfected with HIV and hepatitis C virus (HCV). HIV-RNA was undetectable, and $CD4^+$ cell count was above 500 cells/μl for more than 5 years under the combination of abacavir, nevirapine and lopinavir/ritonavir. In January 2009, lopinavir/ritonavir was replaced with raltegravir because of bleeding tendency related to the use of a protease inhibitor. Abacavir and nevirapine were continued, and no other drugs were modified. The patient visited the hospital on day 18 after the use of raltegravir, complaining of a gradually worsening pain in the right upper abdomen and lower chest wall for 3 days. A nonsteroidal anti-inflammatory drug was not effective, and a computed tomography (CT) scan performed 11 days after the onset of the symptom revealed contrast enhancement of the liver surface (Fig. 1a) and fatty stranding of the greater omentum (Fig. 1b), which are findings compatible with perihepatitis and peritonitis. Oral prednisone (60 mg/day for 3 days, then 30 mg/day for 3 days) was prescribed, and all the symptoms resolved immediately. However, abdominal symptoms developed again after withdrawal of prednisone, necessitating its reintroduction on day 31 at 30 mg/day. Attempts to taper prednisone led to worsening of abdominal pain and development of stomatitis, resulting in continuation of treatment at 20 mg/day. Raltegravir was switched to lopinavir/ritonavir 11 weeks after the onset of abdominal pain and, finally, all antiretroviral drugs were terminated 4 days later because of diarrhea and bleeding related to lopinavir/ritonavir. Abdominal symptoms gradually improved, and prednisone could be tapered to 10 mg/day within 2 weeks. A CT scan performed 10 days after cessation of antiretroviral therapy showed an improvement of perihepatic enhancement. C-reactive protein levels increased to 1.42 mg/dl during raltegravir use and fell to normal levels 6 days after discontinuation of raltegravir. Other laboratory data including transaminase levels showed no changes, and $CD4^+$ cell count and HIV-RNA were stable throughout the course.

This is the first reported case of severe peritonitis associated with raltegravir use. Although not described here, we have experienced several other cases with similar abdominal symptoms that disappeared after raltegravir termination. Several case reports have recently described previously unknown adverse effects related to raltegravir, such as rhabdomyolysis [2] and exacerbation of depression [3]. However, to our knowledge, raltegravir-associated peritonitis has not been reported. In the BENCHMRK

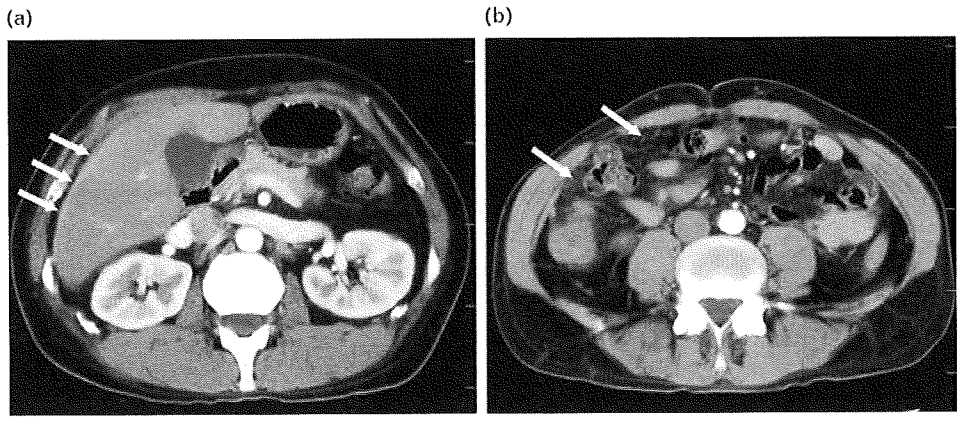

Fig. 1. A computed tomography scan performed 11 days after the onset of the symptoms. A computed tomography scan shows contrast enhancement around the liver surface (a) and fatty stranding of the greater omentum (b).

(Blocking integrase in treatment Experienced patients with a Novel Compound against HIV: MeRcK, MK-0518) study [1], abdominal symptoms, such as diarrhea and nausea, were noted in patients on raltegravir, and some of which might be associated with mild peritonitis.

Fortunately, raltegravir-associated peritonitis seemed reversible, at least to some extent. However, the longer use of raltegravir after onset of symptoms may lead to irreversible and lethal sequelae. Cessation of antiretroviral therapy as a result of severe abdominal symptoms is a potential risk for re-emergence of acute retroviral syndrome or the further accumulation of HIV-resistant mutations.

Whether the described side effects are universal or related to Asians, hemophiliacs or those who have underlying liver disease is unknown at present. Careful monitoring of abdominal symptoms and the consideration of an appropriate radiographic examination are warranted after commencement of raltegravir-containing regimens.

Acknowledgements

The authors thank all clinical staff of the AIDS Clinical Center.

All authors contributed to the conception, design and performance of this submission.

This study was supported in part by the Ministry of Health, Labour, and Welfare of Japan.

All authors report no potential conflict of interests.

Kunihisa Tsukada, Katsuji Teruya, Daisuke Tasato, Hiroyuki Gatanaga, Yoshimi Kikuchi and Shinichi Oka, *AIDS Clinical Center, International Medical Center of Japan, Tokyo, Japan.*

Correspondence to Kunihisa Tsukada, MD, AIDS Clinical Center, International Medical Center of Japan, 1-21-1 Toyama, Shinjuku-ku, Tokyo 162-8655, Japan. Tel: +81 3 3202 7181; fax: +81 3 3202 7198; e-mail: ktsukada@imcj.acc.go.jp

Received: 29 September 2009; accepted: 2 October 2009.

References

1. Steigbigel RT, Cooper DA, Kumar PN, Eron JE, Schechter M, Markowitz M, *et al.* **Raltegravir with optimized background therapy for resistant HIV-1 infection.** *N Engl J Med* 2008; **359**:339–354.
2. Zembower TR, Gerzenshtein L, Coleman K, Palella FJ Jr. **Severe rhabdomyolysis associated with raltegravir use.** *AIDS* 2008; **22**:1382–1384.
3. Harris M, Larsen G, Montaner JS. **Exacerbation of depression associated with starting raltegravir: a report of four cases.** *AIDS* 2008; **22**:1890–1892.

DOI:10.1097/QAD.0b013e328333d28d

The International Journal of Biochemistry & Cell Biology 41 (2009) 891–899

Contents lists available at ScienceDirect

The International Journal of Biochemistry & Cell Biology

journal homepage: www.elsevier.com/locate/biocel

Electrostatically constrained α-helical peptide inhibits replication of HIV-1 resistant to enfuvirtide

Hiroki Nishikawa[a], Shota Nakamura[b], Eiichi Kodama[c,*], Saori Ito[a], Keiko Kajiwara[c,d], Kazuki Izumi[c], Yasuko Sakagami[c], Shinya Oishi[a], Tadayasu Ohkubo[e], Yuji Kobayashi[f], Akira Otaka[g], Nobutaka Fujii[a], Masao Matsuoka[c]

[a] Graduate School of Pharmaceutical Sciences, Kyoto University, Sakyo-ku, Kyoto 606-8501, Japan
[b] Research Institute for Microbial Diseases, Osaka University, Suita, Osaka 565-0871, Japan
[c] Laboratory of Virus Control, Institute for Virus Research, Kyoto University, Sakyo-ku, Kyoto 606-8507, Japan
[d] Institute for Virus Research, and Graduate School of Biostudies, Kyoto University, Sakyo-ku, Kyoto 606-8507, Japan
[e] Graduate School of Pharmaceutical Sciences, Osaka University, Suita, Osaka 565-0871, Japan
[f] Osaka University of Pharmaceutical Sciences, Takatsuki, Osaka 569-1094, Japan
[g] Graduate School of Pharmaceutical Sciences, The University of Tokushima, Tokushima 770-8505, Japan

ARTICLE INFO

Article history:
Received 7 July 2008
Received in revised form 19 August 2008
Accepted 22 August 2008
Available online 10 September 2008

Keywords:
HIV
Fusion
Peptide
Inhibitor
α-Helix

ABSTRACT

α-Helical peptides, such as T-20 (enfuvirtide) and C34, derived from the gp41 carboxyl-terminal heptad repeat (C-HR) of HIV-1, inhibit membrane fusion of HIV-1 and the target cells. Although T-20 effectively suppresses the replication of multi-drug resistant HIV variants both in vitro and in vivo, prolonged therapy with T-20 induces emergence of T-20 resistant variants. In order to suppress the emergence of such resistant variants, we introduced charged and hydrophilic amino acids, glutamic acid (E) and lysine (K), at the solvent accessible site of C34. In particular, the modified peptide, SC34EK, demonstrates remarkably potent inhibition of membrane fusion by the resistant HIV-1 variants as well as wild-type viruses. The activity was specific to HIV-1 and little influenced by serum components. We found a strong correlation between the anti-HIV-1 activities of these peptides and the thermostabilities of the 6-helix bundles that are formed with these peptides. We also obtained the crystal structure of SC34EK in complex with a 36 amino acid sequence (N36) comprising the amino-terminal heptad repeat of HIV-1. The EK substitutions in the sequence of SC34EK were directed toward the solvent and generated an electrostatic potential, which may result in enhanced α-helicity of the peptide inhibitor. The 6-helix bundle complex of SC34EK with N36 appears to be structurally similar to that of C34 and N36. Our approach to enhancing α-helicity of the peptide inhibitor may enable future design of highly effective and specific HIV-1 inhibitors.

1. Introduction

Enfuvirtide (T-20), which has been clinically approved as the first fusion inhibitor of HIV-1, is derived from a 36 amino acid region of the carboxyl-terminal heptad repeat (C-HR) of gp41, an HIV-1 transmembrane envelope glycoprotein, which plays central role in the fusion of HIV-1 with host cells. T-20 prevents the formation of a 6-helix bundle, which is comprised of a trimer of dimers formed from the amino-terminal heptad repeat (N-HR) and the carboxyl-terminal heptad repeat (C-HR) in an antiparallel orientation. Six-helix formation by physiological gp41 enables host cell and virus membranes to contact and fuse, enabling the virus entry into the cells. Therefore, inhibition of the formation of this 6-helix bundle prevents fusion of HIV-1 and targeted host cell membranes (Derdeyn et al., 2000; Wild et al., 1992). Notably, T-20 effectively suppresses the replication of HIV-1 variants, which are resistant to multiple reverse transcriptase and protease inhibitors, and has been used in the optimized regimens for HIV-1-infected patients harboring multi-drug resistant HIV-1 variants (Lalezari et al., 2003; Lazzarin et al., 2003).

Emergence of T-20-resistant HIV-1 was reported not only in patients receiving T-20 monotherapy in a phase I clinical trial (Wei et al., 2002), but also in patients treated with a combination of T-20

* Corresponding author at: 53 Kawaramachi Shogoin, Sakyo-ku, Kyoto 606-8507, Japan. Tel.: +81 75 751 3986; fax: +81 75 751 3986.
E-mail address: ekodama@virus.kyoto-u.ac.jp (E. Kodama).

1357-2725/$ – see front matter © 2008 Elsevier Ltd. All rights reserved.
doi:10.1016/j.biocel.2008.08.039

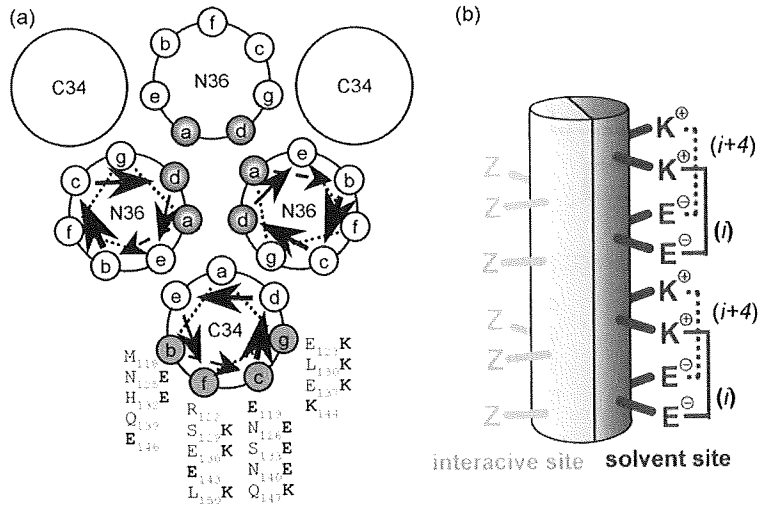

Fig. 1. Helical wheel representation of the 6-helix bundle structure and the design of SC34EK. (a) Amino acid residues at positions a, d, e of C34 are interactive sites that form the 6-helix complex with N36, while the remaining amino acid residues at positions b, c, f, g are solvent accessible sites, which are substituted with Glu (E) or Lys (K) in SC34EK. (b) The design concept of introducing the EK motif to the solvent accessible site. The α-helical C-HR peptide could be divided into interactive (red) and solvent (blue) sites. Z indicates the original amino acids of C34. Only amino acid residues at solvent sites were replaced by E at the *i* position and K at the *i* + 4 position.

and other inhibitors in subsequent phases II and III trials (Matthews et al., 2004; Poveda et al., 2002). These resistant variants frequently acquired mutations in gp41, especially in amino acids 36–45 of the N-HR region (Aquaro et al., 2006; Cabrera et al., 2006; Mink et al., 2005; Poveda et al., 2002; Rimsky et al., 1998; Wei et al., 2002) (Fig. 1). Additionally, complementary mutations in the C-HR region, such as S138A mutation, were found in some T-20 resistant variants (Cabrera et al., 2006; Poveda et al., 2004; Xu et al., 2005). Introduction of these complementary mutations compensates for impaired HIV-1 replication stemming from the primary mutations that give rise to resistance. The N43D mutation in the N-HR region that confers resistance to T-20 is a well documented example (Xu et al., 2005).

Although T-20 inhibits gp41-mediated fusion (Derdeyn et al., 2000; Wild et al., 1992), it has additional effects on HIV-1 replication. For instance, baseline sensitivity of HIV-1 to T-20 is influenced not only by the amino acid sequence of gp41, but also by the co-receptor specificity (CCR5/CXCR4) defined by the structure of the V3 loop of gp120, a glycoprotein capping gp41, which binds to the CD4 cells (Derdeyn et al., 2000; Derdeyn et al., 2001). Moreover, substitutions within the CD4 binding domain of gp120 also contribute to the resistance of the virus to T-20 (Baldwin and Berkhout, 2006). Thus, the mode of action and the mechanism of resistance to T-20 seem to be complicated. In contrast, another fusion inhibitor known as C34, has been clearly shown to bind to the N-HR in vitro and act as a decoy of gp41 C-HR and prevent the formation of the 6-helix bundle (Chan et al., 1997; Liu et al., 2005; Xu et al., 2007). Its inhibitory effect is over 10-fold greater than that of T-20 (Armand-Ugon et al., 2003; Nameki et al., 2005). Thus, C34 appears to be a suitable peptide to employ in the rational design of an improved HIV fusion inhibitor, based on the interaction between the peptide and the target.

It has been reported that α-helicity of the C-HR and N-HR peptide complexes correlates with the anti-HIV-1 activity of the peptide inhibitor (Chan et al., 1998), suggesting that enhancement of α-helicity of C34 may provide higher affinity to the N-HR region, thus resulting in more potent anti-HIV-1 activity. To design potent fusion inhibitors using the enhancement of α-helicity approach, we divided the α-helical peptide C34 into two characteristic interactive (a, d, e) and solvent accessible (b, c, f, g) sites according to the reported N36/C34 structure (Fig. 1) (Chan et al., 1997). When HIV-1 gp41 is folded, a tryptophan-rich domain (WRD) in the N-terminus of C-HR plays an important role in tight and specific binding, through the interaction of the hydrophobic aromatic ring with a deep groove formed by the N-HR coiled coil (Chan and Kim, 1998; Salzwedel et al., 1999). In fact, C34 contains the N-terminal WRD, which binds to a hydrophobic pocket formed by the amino acid residues L57, W60 and K63 on the N-HR trimer surface (Chan et al., 1998; Ferrer et al., 1999), resulting in higher anti-HIV-1 activity of C34 compared to T-20, which lacks the N-terminal WRD. On the other hand, the solvent accessible site appears to contribute little to the formation of the 6-helix bundles, as demonstrated by the crystal structure of C34 bound to N36 (Chan et al., 1997). Therefore, amino acids in the interactive site are indispensable for binding, whereas those in the solvent accessible site may be replaceable (Fig. 1). To enhance the α-helicity of C34, we introduced a series of systematic replacements of amino acid residues in the solvent accessible site, where the original amino acid residues were substituted with charged and hydrophilic glutamic acid (E) or lysine (K) with the intention of forming possible intrahelical salt-bridges (Marqusee and Baldwin, 1987) (Fig. 1b). We obtained two peptides, SC34 and SC34EK (Fig. 2a), both of which gratifyingly demonstrated increased anti-HIV-1 activity (Otaka et al., 2002).

In this study, we demonstrate that SC34EK maintains highly potent activity against T-20 resistant clones of HIV-1, as well as several clinical isolates, and we reveal that the enhanced α-helicity of SC34EK is indeed involved in the improvement of activity. The activities are specific to HIV-1 and are not influenced by serum components. Structural analysis indicates that electrostatic interactions introduced by EK substitutions enhance the conformational stability of the 6-helix bundle, thus preventing HIV-1 fusion with the host cell. The information from our investigations involving the enhanced α-helicity of SC34EK should enable further design of highly effective and specific HIV-1 inhibitors.

2. Materials and methods

2.1. Cells and viruses

MT-2 and 293T cells were grown in RPMI1640- and Dulbecco's modified Eagle medium (DMEM)-based culture medium, respec-

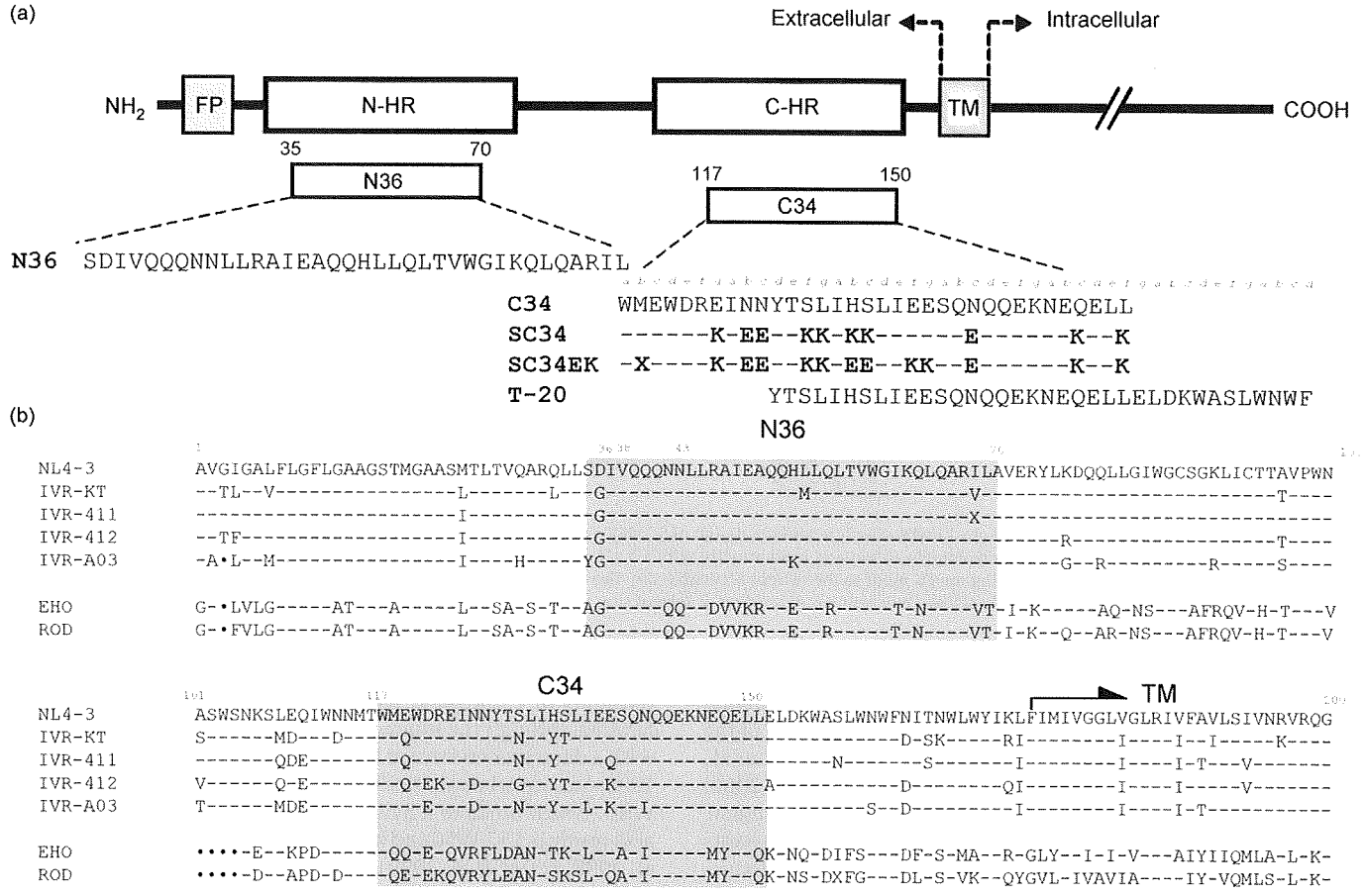

Fig. 2. Schematic view of gp41 and C34 derivatives and amino acid alignment of gp41. (a) The locations of the fusion peptide (FP), the amino-terminal heptad repeat region (N-HR), the carboxyl-terminal heptad repeat region (C-HR), and the transmembrane domain (TM) and the amino acid sequences of N36, T-20, C34 and its derivatives are shown. The residue numbers of each peptide correspond to their positions in gp41 of the NL4-3 strain. The X in SC34EK indicates norleucine, introduced to avoid oxidation of the methionine residues. No differences between the original methionine- and norleucine-containing peptide were observed (Otaka et al., 2002). (b) Alignment of amino acid sequence of clinical isolates (KT, IVR411, IVR412 and IVR-A03; GenBank accession number; AB222704, AB222705, AB222706 and AB222703, respectively) and HIV-2 strains (EHO and ROD) are shown. Corresponding regions of N36 and C34 are indicated in gray. Identical or deleted amino acids from the sequence of NL4-3 are indicated with a bar or a dot, respectively. The X in amino acid sequences of IVR411 and ROD indicates the mixture of I and V for IVR411, and mixture of I and M for ROD.

tively. HeLa-CD4-LTR-β-gal cells were kindly provided by Dr. M. Emerman through the AIDS Research and Reference Reagent Program, Division of AIDS, National Institute of Allergy and Infectious Disease (NIAID) (Bethesda, MD) and were used for the drug susceptibility assay (MAGI assay) as described previously (Kimpton and Emerman, 1992; Kodama et al., 2001; Maeda et al., 1998). The activity of test compounds was determined as the concentration that blocked HIV-1 replication by 50% (EC_{50}).

Laboratory HIV-1 (III_B) and HIV-2 (EHO and ROD) strains were used. An HIV-1 infectious clone pNL4-3 was used for constructions and for the production of HIV-1 variants as described (Nameki et al., 2005). A wild-type HIV-1, HIV-1_{WT}, was generated by transfection of pNL4-3 into 293T cells. Clinical isolates obtained from drug-naïve and heavily drug-experienced patients, were kindly provided by Dr. S. Oka (AIDS Clinical Center, International Medical Center of Japan, Tokyo, Japan). Their co-receptor tropisms were determined using NCK45 cells as described previously (Kajiwara et al., 2006).

2.2. Antiviral agent

The peptide-based fusion inhibitors used in this study were synthesized as described previously (Otaka et al., 2002), and the sequences can be identified in Fig. 2a. 3′-Azido-3′-deoxythymidine (AZT) and 2′,3′-dideoxycytidine (ddC) were purchased from Sigma (St. Louis, MO, USA). MKC-442 was provided by Dr. S. Shigeta (Fukushima Medical University, Fukushima, Japan).

2.3. Determination of drug susceptibility of HIV-1

The peptide sensitivity of infectious clones was determined using the MAGI assay with as described previously (Kodama et al., 2001; Maeda et al., 1998). The activity of test compounds was determined as the concentration that blocks HIV-1 replication by 50% (EC_{50}). For clinical isolates, PHA-stimulated peripheral blood mononuclear cells (PBMCs) were used as described previously (Kodama et al., 2001). PBMCs (10^6 cells/ml) were exposed to test compounds and HIV-1, and were cultured in the presence of interleukin 2 for 7 days. Amounts of p24 protein in the supernatants of the cultures were then determined using the commercially available p24 antigen enzyme linked solvent assay kit.

2.4. Construction of recombinant HIV-1 clone

Recombinant infectious HIV-1 clones with substituted V3 regions, pNL-$V3_{ADA}$ and pNL-$V3_{SF162}$ were generated using pNL4-3. The V3 region, corresponding to n.t. 7029–7249 of pNL4-3, was amplified using primers containing appropriate BglII and NheI restriction enzyme cleavage sites for directional cloning into pBS-

Table 1
Antiviral activity of gp41-derived peptides against gp41 and gp120 V3 recombinant virus[a]

Clone	Tropism[b]	EC_{50} (nM)					
		ddC	N36	T-20	C34	SC34	SC34EK
gp41 recombinant virus							
WT[c]		404 ± 196	180 ± 70	35 ± 17	3.2 ± 0.9	1.4 ± 0.7	0.7 ± 0.3
L33S		289 ± 24	39 ± 11	**>1000**	2.9 ± 0.9	1.3 ± 0.1	0.9 ± 0.3
V38A		714 ± 109	407 ± 76	**402 ± 68**	**96 ± 29**	2.0 ± 0.5	1.1 ± 0.6
V38E		291 ± 57	41 ± 14	**>1000**	**492 ± 85**	**37 ± 12**	**4.3 ± 1.3**
N43K		321 ± 8.5	234 ± 63	114 ± 19	**50 ± 9.5**	2.5 ± 0.3	2.7 ± 0.3
N43D		430 ± 42	461 ± 266	**>1000**	**>100**	**9.0 ± 6.6**	1.0 ± 0.8
D36S/V38M		296 ± 88	178 ± 31	42 ± 6.4	7.2 ± 4.0	1.9 ± 0.1	0.8 ± 0.3
V38E/N42S		273 ± 105	227 ± 20	**>1000**	**322 ± 7.5**	**32 ± 3.1**	3.2 ± 1.0
ΔFNSTW/L33S/N43K[d]		276 ± 39	152 ± 31	**>1000**	**248 ± 56**	2.7 ± 0.3	**4.4 ± 0.5**
ΔFNSTW/D36G/I37K/N126K/L204I[d]		246 ± 67	547 ± 7.8	**754 ± 174**	**67 ± 21**	4.6 ± 0.9	2.9 ± 0.8
gp120 V3 recombinant virus							
V3-ADA	R5	362 ± 102	360 ± 91	**289 ± 19**	6.8 ± 3.3	0.7 ± 0.4	2.0 ± 0.2
V3-SF162[e]	R5	995 ± 219	383 ± 9.9	19 ± 2.8	7.8 ± 3.5	0.5 ± 0.2	0.5 ± 0.2
V3-CH1[f]	R5X4	649 ± 4.5	**2207 ± 42**	16 ± 1	5.6 ± 0.1	1.3 ± 0.1	0.7 ± 0.1
V3-CH2[g]	R5	1515 ± 177	192 ± 13	35 ± 32	3.8 ± 0.1	0.4 ± 0	0.9 ± 0.8

[a] Anti-HIV-1 activity was determined using the MAGI assay. All data represent means ± standard deviation obtained from the results of three independent experiments. Bold indicates over 5-fold increase in EC_{50} value compared to HIV-1_{WT}.

[b] The co-receptor tropism was determined using NCK45 cells as described (Kajiwara et al., 2006).

[c] HIV-1_{NL4-3} served as a wild-type virus.

[d] ΔFNSTW is the deletion of five amino acids at position 364–368 in the gp120 V4 region of HIV-1_{NL4-3} (Nameki et al., 2005). Fusion inhibitor resistant variants used have been previously reported (Armand-Ugon et al., 2003; Nameki et al., 2005).

[e] The V3 region of NL4-3 gp120 was replaced with the corresponding region of HIV-1_{SF162}.

[f] HIV-$1_{V3\text{-}CH1}$ has mutations in the gp120 V3 region of primary isolate HIV-1_{KMT}, where GKI is substituted by GEI.

[g] HIV-$1_{V3\text{-}CH2}$ has mutation in the gp120 V3 region of the primary isolate HIV-1_{KMT}, where GKI is substituted by GQI.

$gp120_{WT}$. The resulting amplified V3 region was subjected to BglII and NheI digestion, subcloned into pBS-$gp120_{WT}$ containing the corresponding region in the DNA fragment of EcoRI–NheI (1510 bp containing gp120 V1, V2 and V3, n.t. 5740–7249 of pNL4-3) and subsequently ligated into pNL4-3. pNL-$V3_{CH1}$ and $V3_{CH2}$, CCR5 and dual (CXCR4 and CCR5) tropic molecular clones, were kindly donated by Dr. Y. Maeda, Kumamoto University (Kumamoto, Japan) (Foda et al., 2001; Maeda et al., 2000).

Recombinant infectious HIV-1 clones carrying various mutations in gp120 and/or gp41 were also generated using pNL4-3. Briefly, the desired mutations were introduced using site directed mutagenesis into the region of pSL-$gp41_{WT}$ flanked by the NheI–BamHI restriction enzyme sites (1220 bp containing gp120 V4, V5 and gp41 ectodomain n.t. 7250–8469 of pNL4-3) (Weiner et al., 1994). After restriction enzyme digestion and purification the NheI–BamHI fragments were ligated into pNL4-3, generating a series of molecular clones with the desired mutations.

Each molecular clone was transfected into 293T cells (10^5 cells/6-well culture plate). After 48 h, MT-2 cells (10^6 cells/well) were added and co-cultured with the 293T cells for an additional 24 h. When an extensive cytopathic effect was observed, the supernatants were harvested and stored at −80 °C for further use.

Table 2
Antiviral activity of gp41-derived peptides against clinical isolates[a]

Strain	EC_{50} (nM)				
	AZT	T-20	C34	SC34	SC34EK
NL4-3 (WT)[b]	2.0	36	3.2	0.36	0.4
KT (WT)[b]	2.0	11	0.2	0.1	0.03
IVR411	**7600**	4.1	0.2	3.1	0.04
IVR412	**9060**	23	7.2	**4.8**	0.1
IVR-A03	**1200**	7.0	**17**	**4.1**	0.7

[a] Anti-HIV-1 activity was determined using the amounts of p24 protein in the supernatants of the PHA-stimulated PBMC cultures using commercially available ELISA kit (Kodama et al., 2001). Bold indicates over 5-fold increase in EC_{50} value compared to HIV-1_{WT}.

[b] HIV-1_{NL4-3} and HIV-1_{KT} served as controls.

2.5. Determination of gp41 amino acid sequence

Nucleotide sequences of the clinical isolates were determined using an automated sequencer. Briefly, DNA was extracted from PBMCs infected with the clinical isolates, subjected to nested PCR for the gp41 coding region, and then directly sequenced as described previously (Nameki et al., 2005).

2.6. Measurement of circular dichroism (CD) spectra

N-HR peptides (N36, $N36_{V38A}$ or $N36_{N43D}$) and C-HR peptides (C34 or SC34EK) were incubated at 37 °C for 30 min (the final concentration of both the N-HR peptide and the C-HR peptide were 10 μM in pH 7.4, 12 mM phosphate-buffered solution containing 50 mM NaCl). The wavelength-dependence of molar ellipticity [θ] was monitored at 25 °C as the average of eight scans, and the thermal stability was estimated by monitoring the change in the CD signal at 222 nm in a spectropolarimeter (Model J-710; Jasco, Tokyo, Japan) equipped with a thermoelectric temperature controller. The midpoint of thermal unfolding transition (melting temperature [T_m]) of each complex was determined as described previously (Otaka et al., 2002). The percentages of a-helicity in 6-helix complexes were calculated by comparing the CD signal at 222 nm of N36/C34 or N36/SC34EK complexes in a spectropolarimeter.

2.7. Crystallization, data collection and refinement

Samples for crystallization were prepared by mixing solutions of N36 and SC34EK dissolved in 10 mM sodium acetate buffer at a concentration of 10 mg/mL. The mixture was incubated for 30 min at 37 °C, then was passed through a 22 μm filter. Crystallization was performed by the hanging drop vapor diffusion method at 4 °C. Droplets were prepared of equal amounts (2 μL) of reservoir solution and the peptide solution. Hexagonal prism crystals were obtained under the following conditions: 100 mM sodium acetate buffer (pH 4.0), 200 mM ammonium sulphate, 14% polyethylene glycol monomethyl ether 2000. After screening of

Table 3
Antiviral activity of HIV-1 gp41-derived peptides against HIV-2[a]

HIV-2 strain	EC_{50} (nM)				
	ddC	T-20	C34	SC34	SC34EK
WT[b]	404 ± 196	35 ± 17	3.2 ± 0.9	1.4 ± 0.7	0.7 ± 0.3
$HIV\text{-}2_{EHO}$[c]	925 ± 188	14 ± 3.0 (×0.4)	**639 ± 87 (×200)**	**68 ± 10 (×49)**	**17 ± 1.2** (×24)
$HIV\text{-}2_{ROD}$[d]	**1808 ± 927**	**176 ± 68 (×5)**	**>1000 (>×313)**	**251 ± 29 (×179)**	**115 ± 33** (×164)

[a] Anti-HIV-2 activity was determined using the MAGI assay. All data represent mean ± standard deviation obtained from the results of three independent experiments. Bold indicates over 5-fold increase in EC_{50} value compared to $HIV\text{-}1_{WT}$.
[b] $HIV\text{-}1_{NL4\text{-}3}$ served as a wild-type virus.
[c] $HIV\text{-}2_{EHO}$ was dual-tropic HIV-2.
[d] $HIV\text{-}2_{ROD}$ was T-tropic HIV-2.

various cryo-conditions, the suitable condition was found to be the addition of 35% xylitol to the peptide solution and a slight increase in the amount of the precipitant (*ca* 14.5%). The obtained crystals were easily broken by direct transfer from the crystallization condition to the cryo-condition, but the transfer of the fragile crystals could be accomplished by gradual change in conditions using stepwise increase in the amount (0–35% in five steps) of the cryoprotectant.

Data were collected at a beamline BL38B1 of SPring-8. Collected data were processed using DENZO and SCALEPACK from the HKL2000 package (Otwinowski and Minor, 1997). A molecular replacement solution was found using AMoRe (Navaza, 2001), with a molecular model of the HIV-1 gp41 core structure (PDB code: 1AIK). Model refinements and reconstruction were performed using REFMAC5 (Murshudov et al., 1999) and XtalView (McRee, 1999). The final model was refined at a resolution of 2.1 Å, to a crystallographic *R* value of 0.213 and a free *R* value of 0.238. Detailed data collection and refinement statistics are summarized in Table 1. Atomic coordinates and structural factors have been deposited at the Protein Data Bank (PDB code:2Z2T).

3. Results

3.1. Anti-HIV-1 activity of SC34 and SC34EK

We examined the anti-HIV-1 activity of SC34 and SC34EK against not only $HIV\text{-}1_{WT}$ but also T-20- and/or C34-resistant clones observed in vitro. SC34 and especially SC34EK that has aligned EK modification more effectively suppress HIV-1 infection compared to C34 and T-20 (Table 1). D36S/V38M substitutions in the gp41 region ($HIV\text{-}1_{D36S/V38M}$), and a five amino acid (FNSTW) deletion in the V4 region of gp120 (ΔV4) with L33S/N43K in the gp41 region ($HIV\text{-}1_{\Delta V4/L33S/N43K}$) were isolated in vitro (Fikkert et al., 2002; Rimsky et al., 1998). L33S was also selected during C34-resistant induction in vitro (Armand-Ugon et al., 2003). C34 and its derivatives effectively inhibit entry of these clones into the host cell. In particular, SC34EK maintained strong activity even against V38E containing clones, such as $HIV\text{-}1_{V38E/N42S}$ (Armand-Ugon et al., 2003), which showed cross-resistance to T-20, C34 and SC34. Reduction of activities by SC34 and SC34EK was moderate in $HIV\text{-}1_{\Delta FNSTW/L33S/N43K}$ that showed high level resistance to T-20 and C34. Next, we examined the antiviral activities of C34 derivatives against clones containing major primary mutations V38A and N43D, which are mutations frequently observed in T-20 resistant variants in vivo (Cabrera et al., 2006; Derdeyn et al., 2001; Menzo et al., 2004; Poveda et al., 2004; Poveda et al., 2002; Xu et al., 2005) (Table 1). SC34 reduced its antiviral activities against $HIV\text{-}1_{N43D}$, while SC34EK maintained its potent activity, indicating that when EK is bound with the complementary electrostatic interactions appropriately aligned SC34EK can effectively suppress the infection by various clones resistant to T-20 and C34 both in vitro and in vivo.

We further evaluated activities of SC34 and SC34EK against V3-substituted clones (Table 1). $HIV\text{-}1_{V3\text{-}ADA}$ uses mainly the CCR5 co-receptor for its entry into the host cells and has been reported to moderate T-20 resistance (≈10 fold), compared to the CXCR4 using strain of HIV-1, which shows higher susceptibility to fusion inhibitors (Reeves et al., 2002). As reported, the susceptibility of $HIV\text{-}1_{V3\text{-}ADA}$ to T-20 decreased, however, C34 and its derivatives maintained their activity against the same variant. Interestingly, in our experiments, $HIV\text{-}1_{V3\text{-}SF162}$, $HIV\text{-}1_{V3\text{-}CH1}$ and $HIV\text{-}1_{V3\text{-}CH2}$ also showed comparable susceptibility to T-20. These results indicate that sequence variations in the V3 region do not always correlate with the observed T-20 susceptibility and are not involved in the resistance to C34 and its derivatives.

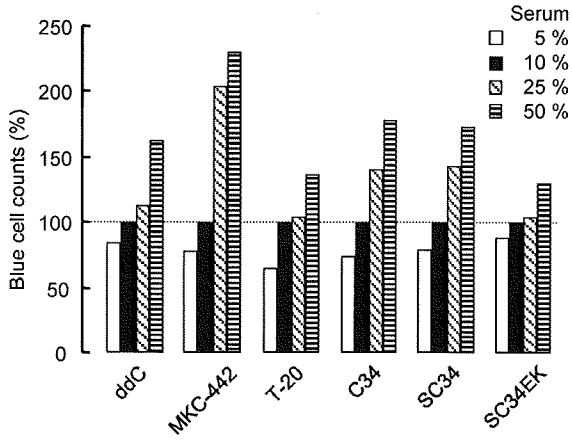

Fig. 3. Effect of FCS concentrations on anti-HIV-1 activity. Changes in the blue cell counts at various concentrations of FCS are shown. Blue cell counts at EC_{80} value in 10% FCS concentration (black bar) were used and set as 100%. White, black, hatched, and striped bars correspond to 5, 10, 25, and 50% FCS, respectively. Inhibitors for reverse transcriptase, ddC and MKC-442, and for fusion, T-20 were used as controls.

3.2. Amino acid sequence

Amino acid sequences of clinical isolates are shown in Fig. 2b. One isolate, $HIV\text{-}1_{KT}$, was obtained from a drug-naïve patient and the other three isolates ($HIV\text{-}1_{411}$, $HIV\text{-}1_{412}$, $HIV\text{-}1_{A03}$) were obtained from heavily drug-experienced patients. None of the patients had received T-20 therapy. Amino acid sequences of the N-HR were highly conserved within all HIV-1 clinical isolates with some small variations. In contrast, the N36 region of the two HIV-2 strains, EHO and ROD, was identical in both HIV-2 isolates. We found some variations in the amino acid sequences of the HIV-2 strains we isolated, as compared with the sequences deposited in the GenBank (accession number; M15390 and X05291 for $HIV\text{-}2_{ROD}$, and U272000 for $HIV\text{-}2_{EHO}$). Namely, we identified two different amino acids in the isolated $HIV\text{-}2_{ROD}$, V26L and

I157I/M (mixture of I and M), and one variation in the amino acid sequence of HIV-2_{EHO}, V45L. Except for I157M, other substitutions are observed in the majority of the HIV-2 strains, as reported in the HIV sequence database (Los Alamos National Laboratory: Los Alamos, NM, USA, http://www.hiv.lanl.gov). These substitutions might be introduced through different culture conditions, (e.g., host cells used for the propagation). We considered these substitutions as a polymorphism.

Sequence homology of the N36 region of the isolated HIV-1 strains was 31/36 (86%), including mutation D36G that is observed in the vast majority of HIV-1 strains (Kuiken et al., 2001). In contrast, those of the C34 region were relatively heterogeneous, 24/34 (71%) for HIV-1 and 12/34 (35%) for HIV-2. Sequence identity of the T-20 region (residues 117–152) in the HIV-1 strains was also variable 27/36 (75%), while in the HIV-2 strains the sequence identity was 15/36 (42%). These results indicate that even highly conserved two helical extracellular domain of the gp41 can allow polymorphisms.

3.3. Efficacy of the peptides against clinical isolates

To evaluate preclinical efficacy, we examined the antiviral activity of C34, SC34 and SC34EK against clinical isolates (Table 2). Replication of HIV-1_{NL4-3} and HIV-1_{KT}, a drug-naïve strain, was suppressed by all compounds tested. C34 showed decreased activity against HIV-$1_{IVR-A03}$, which was isolated from a heavily drug-exposed patient. SC34 also showed reduced susceptibility against three drug-experienced strains. However, it is difficult to conclude whether SC34 showed enhanced susceptibility against HIV-1_{KT} or reduced susceptibility against drug resistant strains. In contrast, T-20 and SC34EK suppressed the replication of all isolates tested to similar extents in EC_{50} values compared to HIV-1_{NL4-3} (Table 2), indicating that SC34EK with appropriately aligned EK residues effectively suppresses the replication of the clinical 3 isolates.

3.4. Anti-HIV-2 activity

To confirm the target specificity, we examined antiviral activities of SC34 and SC34EK against two HIV-2 strains, EHO and ROD. Compared to HIV-1_{NL4-3}, EHO and ROD contain 19 and 22 amino acid substitutions in the C34 region, respectively, and 15 amino acid substitutions in the N36 region, the anticipated site of binding of SC34 and SC34EK peptides (Fig. 2b). Like the parent peptide C34, both SC34 and SC34EK lost their potent activities (Table 3). Compared to HIV-1_{NL4-3}, 6 out of 19 residues in the C34 region of HIV-2_{EHO} and 7 out of 22 residues in the C34 region of HIV-2_{ROD} are located at positions *a*, *d*, and *e* that directly interact with the N36 binding surface. These substitutions in the N36 and C34 region in HIV-2 may be responsible for reduced anti-HIV-2 activities of the peptides derived from HIV-1. At present, we cannot conclude which amino acid substitutions are directly involved in the reduced susceptibility of the HIV-2 strain to the treatment with the peptide fusion inhibitor, and/or whether other regions besides the N36 and C34 regions might influence peptide susceptibility. However, our results indicate that SC34 and SC34EK maintain similar target specificity to the parent peptide, C34.

3.5. Effect of fetal calf serum (FCS) on anti-HIV-1 activity

To estimate the stability of the peptides in vivo, binding level of SC34EK, to serum components, (e.g., albumin) was examined. In this experiment, the antiviral activity in the presence of relatively high concentrations of fetal calf serum (FCS) was determined (Baba et al., 1993) (Fig. 3). EC_{80} values of the fusion inhibitors against HIV-1 replication in vitro were used. In the presence of 50% FCS, the activity of MKC-442 (I-EBU), a lipophilic non-nucleoside RT inhibitor, was reduced 2.3-fold compared with 10% FCS as described previously (Baba et al., 1993). However, the activities of SC34, SC34EK and T-20 were little influenced by serum components. Among the three, SC34EK was the least affected by the concentration of FCS.

We further examined the stability of peptide inhibitors in freshly prepared human sera ($n = 3$). After 1 h incubation of peptides in human sera (final concentration of 200 μM) at 37 °C, the anti-HIV-1 activity was examined using the MAGI assay. Comparable activities of all peptides tested were observed either with or without the incubation (data not shown). These results indicate that hydrophilic SC34EK likely retains its strong anti-HIV-1 activity in vivo, similarly to T-20, because of its low non-specific binding and protease cleavage in serum.

3.6. Peptide binding affinity

To clarify the mechanism of potent anti-HIV-1 activity observed with SC34EK, the binding affinity of SC34EK was evaluated by collecting the CD spectra using synthetic peptides. The CD spectra of equimolar mixtures of the N-HR and C-HR peptides showed spectrum minima at 208 and 222 nm, which indicate the presence of stable α-helical conformations. All combinations of peptides showed similar spectra at 25 °C, indicating that these peptides contained the same α-helicity (Fig. 4a), although the spectrum of C34 with N36 and N43D mutation ($N36_{N43D}$) indicated only weak α-helicity. These results indicate that N43D might reduce the stability of the conformation of the 6-helix bundle, thus decreasing the replication of HIV-1, whereas V38A does not. SC34EK formed stable 6-helix conformations with $N36_{V38A}$ and $N36_{N43D}$. Under these experimental conditions, wavelength-dependent spectra were similar with the exception of the spectrum of the $N36_{N43D}$/C34 complex. Thus, we analyzed thermal stabilities, defined as the midpoint of the thermal unfolding transition (T_m) values, of the potential 6-helix bundles of N-HR and C-HR peptides. T_m of N36/C34 was found to be 52.0 °C, while that of $N36_{V38A}$/C34 and $N36_{N43D}$/C34 decreased to 44.5 and 34.0 °C, respectively (Fig. 3b). In contrast, thermal stabilities of $N36_{V38A}$/SC34EK, $N36_{N43D}$/SC34EK and N36/SC34EK were much higher, 60.5, 56.0 and 69.5 °C, respectively. Thus, binding affinity of SC34EK to N-HR was stronger compared to that of C34. Alternatively, at the physiological temperature of 37 °C, only 60 and 40% of the α-helix content was observed in $N36_{V38A}$/C34 and $N36_{N43D}$/C34 mixtures, respectively, indicating that roughly half of C34 failed to form stably 6-helix bundle with the target N-HR harboring resistant mutations. Therefore, C34 reduces its anti-fusion activity exerted by dominant negative effect. In contrast, only 20% of the unfolded α-helix content was observed in SC34EK with mutated N36, which indicated that at 37 °C, binding of SC34EK to mutated N36 was comparable to that of C34 with wild-type N36 (Fig. 4b). Moreover, physiochemical properties of N-HR and SC34EK complexes, defined by T_m value, correlated well with their ability to inhibit HIV-1 fusion (Fig. 4c). These results suggest that the stability of the 6-helix complex, as judged by the binding stability (affinity), is directly correlated with the anti-HIV-1 activity.

3.7. Crystal structure of the N36/SC34EK complex

The crystal structure of the complex between SC34EK and the N-HR representative peptide N36 was resolved to a resolution of 2.1 Å (Table 4). In the asymmetric unit, a 6-helix bundle consisting of a central helix bundle of three N36 peptides surrounded by three SC34EK peptides was found. This arrangement is similar in the core structure of gp41 (Chan et al., 1997). Structural superimposition of the original gp41 core and the N36/SC34EK complex showed a good match, with an RMSD value of 0.59 for main-chain atoms

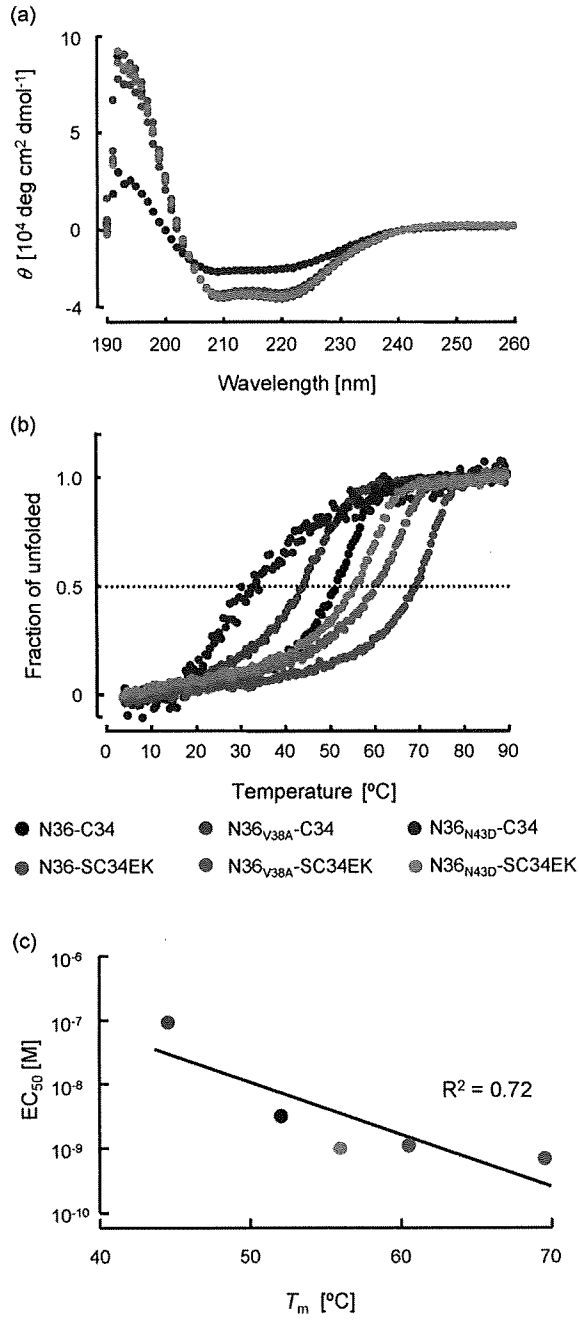

Fig. 4. CD analysis of peptide complex between resistant variants of N36 and C34 or SC34EK. (a) Wavelength-dependent CD spectra of the complexes in solution. The spectrum minima at 208 and 222 nm indicated the presence of stable α-helical conformations. (b) Thermal midpoint analysis was measured at 222 nm CD signal for the N and C peptide complexes. Final concentration of each peptide was 10 mM. The arrow indicates the physiological temperature of 37 °C. (c) The correlation between T_m (b) and EC_{50} values (Table 1). Colors of plots correspond to those in panels (a) and (b). Combination of $N36_{N43D}$ and C34 (EC_{50} > 100 nM) is excluded.

(Fig. 5a and b). Hydrophobic contacts between SC34EK and N36 with tryptophan rich domain (WRD) and leucine zipper were preserved for the original gp41 core. All introduced charged residues of the EK motif were directed toward the solvent (Fig. 5c). As a direct consequence of introducing the EK motifs, the ratio of surface area occupied by charged residues to the total surface area was increased from 35% in the original molecule to 60% in the N36/SC34EK complex. Importantly, it appeared that tight bonding, such as ion pairing or hydrogen bonding, was not present in the

Table 4
Crystallization, data collection and refinement statistics

Data collection	BL38B1 Spring-8
Temperature (K)	100
Space group	$P3_121$
Cell dimensions *a*, *b*, *c* (Å)	105.01, 105.01, 78.31
Resolution limits (Å)	90.00–2.10
Number of unique reflections	29,461
Average redundancy	7.53
Completeness (%)	99.7
R_{merge}[a]	0.122
Refinement statistics	
Refinements resolution range (Å)	20.00–2.20
R/R_{free}[b] (%)	0.213/0.238
The highest resolution shell (Å)	2.15–2.10
R/R_{free}[b] (%)	0.231/0.255
RMSD from ideal	
Bonds (Å)	0.010
Angles (°)	1.015
⟨*B*⟩ for atomic model[c] (Å²)	29.93
Ramachandran plot	
Most favored regions (%)	100

[a] $R_{merge} = \sum|I_h - \langle I_h\rangle|/\sum I_h$, where $\langle I_h\rangle$ is the average intensity of reflection *h* and symmetry-related reflections.

[b] *R* and $R_{free} = \sum||F_o| - |F_c||/\sum|F_o|$ calculated for reflections of the working set and test (5%) set, respectively.

[c] ⟨*B*⟩ is the average temperature factor for all protein atoms.

side-chains of the residues of the EK motif. Electrostatic interaction may involve in constrained structure which provides the enhanced α-helicity observed (Fig. 4). This structural analysis demonstrated that the interaction between N36 and SC34EK retained the ability to form the 6-helix bundle structure despite the substitution of more than one third of the residues (13/34) in the sequence of SC34EK.

4. Discussion

In this study, we characterized a novel α-helical peptide, SC34EK that effectively inhibits replication of HIV-1 strains resistant to T-20 and C34. The activity was specific to HIV-1 and little influenced by serum components. We demonstrate that the potent anti-HIV-1 activity of SC34EK is derived from its high affinity to the N-HR region by the CD analysis. Further, we reveal that SC34EK binds to its target, N-HR in identical manner that C34 does by the structure analysis.

The structural analysis of the N36/SC34EK complex clearly demonstrated that the interaction between SC34EK and N36 peptides was maintained by hydrophobic contacts and that the EK motif was directed toward the solvent. The introduction of the EK residues increased the proportion of accessible surface area occupied by charged residues. Although tight bonding was not observed, a continuous electrostatic potential between the EK residues may serve to stabilize the helix bundle. Such helix stabilization, which might occur on the surface of the HIV-1 virion between SC34EK and the N36 region of gp41, could result in the high anti-HIV-1 activity. In this regard, SC34EK, containing an aligned EK motif, showed more potent anti-HIV-1 activity compared to SC34, which has one misaligned EK motif (Fig. 2a). Increasing the hydrophilic surface area may prevent aggregation of SC34EK as compared to parental peptide C34. Therefore, SC34EK might distribute into the various organs in the body without being trapped and destroyed in the reticular systems or having its activity reduced by non-specific binding to proteins (e.g., albumin) (Fig. 3).

We further demonstrate that SC34EK specifically binds to the target, N-HR of HIV-1, since it only exerted weak activity to two

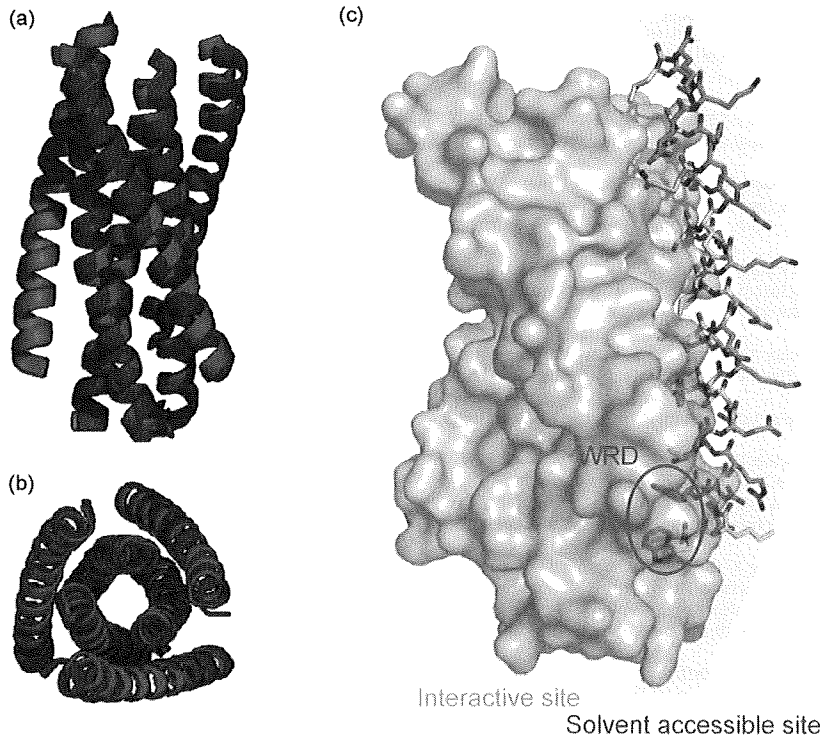

Fig. 5. Structure of the 6-helix bundle formed by N36 and SC34EK. (a and b) The gp41 core structure and N36/SC34EK complex are shown in red and blue, respectively. (c) Stick model representation of SC34EK. The stick model of SC34EK is shown, and three N36s in the core and two other surrounded SC34EK are represented in gray. SC34EK showed amphiphilic properties. The location of the N-terminal tryptophan rich domain (WRD) in SC34EK is indicated by a red circle. Original and introduced charged amino acids are indicated in green and blue, respectively.

HIV-2 strains that contain 15 amino acid substitutions in the N-HR compared to HIV-1 NL4-3 strain (Table 3 and Fig. 2b). These results suggest that to develop resistance to SC34EK, at least, certain mutations in not only the N-HR but also the C-HR are required to be introduced. This might delay emergence of resistant HIV-1 variants to SC34EK in vivo.

So far, some approaches for stabilizing α-helix structures through the introduction of artificial amino acids were reported for HIV-1 fusion inhibitors T-20 (Judice et al., 1997) and C34 (Sia et al., 2002), including an example of an amino acid containing terminal olefin-derived side chains, designed as a substrate for the ring-closing olefin metathesis (Blackwell et al., 2001) and an example of a hydrocarbon-stapled peptides (Phelan et al., 1997) Walensky et al. (2004) applied a hydrocarbon-stapled modification to generate peptides that bind to the BH3 helical domain of Bcl-2, an anti-apoptotic protein, and demonstrated that a synthesized peptide mimic that binds to the BH3 domain activates apoptosis in leukemic cells. However, all peptides exerted only moderate activity in vivo, although they showed efficient binding to the target proteins in vitro (Blackwell et al., 2001; Judice et al., 1997; Sia et al., 2002; Walensky et al., 2004). It is likely that during the formation of the 6-helix bundle and the fusion process, gp41 changes its conformation drastically, suggesting that a flexible conformation of the peptide may be required to preserve actual inhibition. Compared with tethered, constrained peptides, EK modification that facilitates electrostatic stabilization displays such flexibility while exhibiting enhanced α-helicity. Most recently, T290676, a 38 amino acid peptide, has been reported to suppress various fusion inhibitor-resistant strains of HIV-1 (Dwyer et al., 2007). Like SC34EK, T290676 is substituted with the charged and hydrophilic amino acids, glutamic acid (E) and arginine (R), at the solvent accessible site and shows potent anti-HIV-1 activity.

In conclusion, we have demonstrated that SC34EK selectively inhibits various HIV-1 strains, including T-20 resistant clones, through increased stability of the α-helix. The sequence of the solvent accessible site of α-helical peptides is replaceable and modifications of this sequence can regulate α-helicity with target specificity. Therefore, our approach of introducing the EK motif in the α-helical structure of the peptide inhibitor will help to generate future peptide inhibitors with high anti-HIV efficacy and potentially fewer adverse effects.

Acknowledgements

This work was supported in part by grants for the Promotion of AIDS Research from the Ministry of Health and Welfare and for the Ministry of Education, Culture, Sports, Science, and Technology (MEXT) of Japan (E.K. and S.O.); a grant for Research for Health Sciences Focusing on Drug Innovation from the Japan Health Sciences Foundation (E.K., S.O., N.F. and M.M.), the Program of Founding Research Centers for Emerging and Reemerging Infectious Diseases by the MEXT (S.N.), a Health and Labor Sciences Research Grant for Research on HIV/AIDS from the Ministry of Health and Labor of Japan (S.N.), and the 21st Century COE program (H.N., K.K., K.I. and N.F.). H.N. is grateful for the JSPS Research Fellowships for Young Scientists. Appreciation is expressed to Mr. Maxwell Reback (Kyoto University) for reading this manuscript.

References

Aquaro S, D'Arrigo R, Svicher V, Perri GD, Caputo SL, Visco-Comandini U, et al. Specific mutations in HIV-1 gp41 are associated with immunological success in HIV-1-infected patients receiving enfuvirtide treatment. J Antimicrob Chemother 2006;58:714–22.

Armand-Ugon M, Gutierrez A, Clotet B, Este JA. HIV-1 resistance to the gp41-dependent fusion inhibitor C-34. Antiviral Res 2003;59:137–42.

Baba M, Yuasa S, Niwa T, Yamamoto M, Yabuuchi S, Takashima H, et al. Effect of human serum on the in vitro anti-HIV-1 activity of 1-[(2-hydroxyethoxy)methyl]-6-(phenylthio)thymine (HEPT) derivatives as related to their lipophilicity and serum protein binding. Biochem Pharmacol 1993;45:2507–12.

Baldwin CE, Berkhout B. Second site escape of a T20-dependent HIV-1 variant by a single amino acid change in the CD4 binding region of the envelope glycoprotein. Retrovirology 2006;3:84.

Blackwell HE, Sadowsky JD, Howard RJ, Sampson JN, Chao JA, Steinmetz WE, et al. Ring-closing metathesis of olefinic peptides: design, synthesis, and structural characterization of macrocyclic helical peptides. J Org Chem 2001;66: 5291–302.

Cabrera C, Marfil S, Garcia E, Martinez-Picado J, Bonjoch A, Bofill M, et al. Genetic evolution of gp41 reveals a highly exclusive relationship between codons 36, 38 and 43 in gp41 under long-term enfuvirtide-containing salvage regimen. AIDS 2006;20:2075–80.

Chan DC, Chutkowski CT, Kim PS. Evidence that a prominent cavity in the coiled coil of HIV type 1 gp41 is an attractive drug target. Proc Natl Acad Sci U S A 1998;95:15613–7.

Chan DC, Fass D, Berger JM, Kim PS. Core structure of gp41 from the HIV envelope glycoprotein. Cell 1997;89:263–73.

Chan DC, Kim PS. HIV entry and its inhibition. Cell 1998;93:681–4.

Derdeyn CA, Decker JM, Sfakianos JN, Wu X, O'Brien WA, Ratner L, et al. Sensitivity of human immunodeficiency virus type 1 to the fusion inhibitor T-20 is modulated by coreceptor specificity defined by the V3 loop of gp120. J Virol 2000;74:8358–67.

Derdeyn CA, Decker JM, Sfakianos JN, Zhang Z, O'Brien WA, Ratner L, et al. Sensitivity of human immunodeficiency virus type 1 to fusion inhibitors targeted to the gp41 first heptad repeat involves distinct regions of gp41 and is consistently modulated by gp120 interactions with the coreceptor. J Virol 2001;75: 8605–14.

Dwyer JJ, Wilson KL, Davison DK, Freel SA, Seedorff JE, Wring SA, et al. Design of helical, oligomeric HIV-1 fusion inhibitor peptides with potent activity against enfuvirtide-resistant virus. Proc Natl Acad Sci U S A 2007;104: 12772–7.

Ferrer M, Kapoor TM, Strassmaier T, Weissenhorn W, Skehel JJ, Oprian D, et al. Selection of gp41-mediated HIV-1 cell entry inhibitors from biased combinatorial libraries of non-natural binding elements. Nat Struct Biol 1999;6: 953–60.

Fikkert V, Cherepanov P, Van Laethem K, Hantson A, Van Remoortel B, Pannecouque C, et al. env chimeric virus technology for evaluating human immunodeficiency virus susceptibility to entry inhibitors. Antimicrob Agents Chemother 2002;46:3954–62.

Foda M, Harada S, Maeda Y. Role of V3 independent domains on a dual-tropic human immunodeficiency virus type 1 (HIV-1) envelope gp120 in CCR5 coreceptor utilization and viral infectivity. Microbiol Immunol 2001;45: 521–30.

Judice JK, Tom JY, Huang W, Wrin T, Vennari J, Petropoulos CJ, et al. Inhibition of HIV type 1 infectivity by constrained alpha-helical peptides: implications for the viral fusion mechanism. Proc Natl Acad Sci U S A 1997;94:13426–30.

Kajiwara K, Kodama E, Matsuoka M. A novel colorimetric assay for CXCR4 and CCR5 tropic human immunodeficiency viruses. Antivir Chem Chemother 2006;17:215–23.

Kimpton J, Emerman M. Detection of replication-competent and pseudotyped human immunodeficiency virus with a sensitive cell line on the basis of activation of an integrated beta-galactosidase gene. J Virol 1992;66: 2232–9.

Kodama EI, Kohgo S, Kitano K, Machida H, Gatanaga H, Shigeta S, et al. 4′-Ethynyl nucleoside analogs: potent inhibitors of multidrug-resistant human immunodeficiency virus variants in vitro. Antimicrob Agents Chemother 2001;45: 1539–46.

Kuiken C, Foly B, Hahn B, Marx P, McCutchan F, Mellors J, et al.Kuiken C, Foly B, Hahn B, Marx P, McCutchan F, Mellors J, Wolinsky S, Korber B, editors. HIV Sequence Compendium 2001. Los Alamos, NM: Los Alamos National Laboratory; 2001.

Lalezari JP, Henry K, O'Hearn M, Montaner JS, Piliero PJ, Trottier B, et al. Enfuvirtide, an HIV-1 fusion inhibitor, for drug-resistant HIV infection in North and South America. N Engl J Med 2003;348:2175–85.

Lazzarin A, Clotet B, Cooper D, Reynes J, Arasteh K, Nelson M, et al. Efficacy of enfuvirtide in patients infected with drug-resistant HIV-1 in Europe and Australia. N Engl J Med 2003;348:2186–95.

Liu S, Lu H, Niu J, Xu Y, Wu S, Jiang S. Different from the HIV fusion inhibitor C34, the anti-HIV drug fuzeon (T-20) inhibits HIV-1 entry by targeting multiple sites in gp41 and gp120. J Biol Chem 2005;280:11259–73.

Maeda Y, Foda M, Matsushita S, Harada S. Involvement of both the V2 and V3 regions of the CCR5-tropic human immunodeficiency virus type 1 envelope in reduced sensitivity to macrophage inflammatory protein 1alpha. J Virol 2000;74:1787–93.

Maeda Y, Venzon DJ, Mitsuya H. Altered drug sensitivity, fitness, and evolution of human immunodeficiency virus type 1 with pol gene mutations conferring multi-dideoxynucleoside resistance. J Infect Dis 1998;177:1207–13.

Marqusee S, Baldwin RL. Helix stabilization by Glu-.Lys+ salt bridges in short peptides of de novo design. Proc Natl Acad Sci U S A 1987;84:8898–902.

Matthews T, Salgo M, Greenberg M, Chung J, DeMasi R, Bolognesi D. Enfuvirtide: the first therapy to inhibit the entry of HIV-1 into host CD4 lymphocyte. Nat Rev Drug Discov 2004;3:215–25.

McRee DE. XtalView/Xfit—a versatile program for manipulating atomic coordinates and electron density. J Struct Biol 1999;125:156–65.

Menzo S, Castagna A, Monachetti A, Hasson H, Danise A, Carini E, et al. Genotype and phenotype patterns of human immunodeficiency virus type 1 resistance to enfuvirtide during long-term treatment. Antimicrob Agents Chemother 2004;48:3253–9.

Mink M, Mosier SM, Janumpalli S, Davison D, Jin L, Melby T, et al. Impact of human immunodeficiency virus type 1 gp41 amino acid substitutions selected during enfuvirtide treatment on gp41 binding and antiviral potency of enfuvirtide in vitro. J Virol 2005;79:12447–54.

Murshudov GN, Vagin AA, Lebedev A, Wilson KS, Dodson EJ. Efficient anisotropic refinement of macromolecular structures using FFT. Acta Crystallogr 1999;D55:247–55.

Nameki D, Kodama E, Ikeuchi M, Mabuchi N, Otaka A, Tamamura H, et al. Mutations conferring resistance to human immunodeficiency virus type 1 fusion inhibitors are restricted by gp41 and Rev-responsive element functions. J Virol 2005;79:764–70.

Navaza J. Implementation of molecular replacement in AMoRe. Acta Crystallogr 2001;D57(Pt 10):1367–72.

Otaka A, Nakamura M, Nameki D, Kodama E, Uchiyama S, Nakamura S, et al. Remodeling of gp41-C34 peptide leads to highly effective inhibitors of the fusion of HIV-1 with target cells. Angew Chem Int Ed Engl 2002;41:2937–40.

Otwinowski Z, Minor W. Processing of X-ray diffraction data collected in oscillation mode. Met Enzymol 1997;276:307–26.

Phelan JC, Skelton NJ, Braisted AC, McDowell RS. A general method for constraining short peptides to an alpha-helical conformation. J Am Chem Soc 1997;119:455–60.

Poveda E, Rodes B, Labernardiere JL, Benito JM, Toro C, Gonzalez-Lahoz J, et al. Evolution of genotypic and phenotypic resistance to Enfuvirtide in HIV-infected patients experiencing prolonged virologic failure. J Med Virol 2004;74:21–8.

Poveda E, Rodes B, Toro C, Martin-Carbonero L, Gonzalez-Lahoz J, Soriano V. Evolution of the gp41 env region in HIV-infected patients receiving T-20, a fusion inhibitor. AIDS 2002;16:1959–61.

Reeves JD, Gallo SA, Ahmad N, Miamidian JL, Harvey PE, Sharron M, et al. Sensitivity of HIV-1 to entry inhibitors correlates with envelope/coreceptor affinity, receptor density, and fusion kinetics. Proc Natl Acad Sci U S A 2002;99:16249–54.

Rimsky LT, Shugars DC, Matthews TJ. Determinants of human immunodeficiency virus type 1 resistance to gp41-derived inhibitory peptides. J Virol 1998;72:986–93.

Salzwedel K, West JT, Hunter E. A conserved tryptophan-rich motif in the membrane-proximal region of the human immunodeficiency virus type 1 gp41 ectodomain is important for Env-mediated fusion and virus infectivity. J Virol 1999;73:2469–80.

Sia SK, Carr PA, Cochran AG, Malashkevich VN, Kim PS. Short constrained peptides that inhibit HIV-1 entry. Proc Natl Acad Sci U S A 2002;99:14664–9.

Walensky LD, Kung AL, Escher I, Malia TJ, Barbuto S, Wright RD, et al. Activation of apoptosis in vivo by a hydrocarbon-stapled BH3 helix. Science 2004;305:1466–70.

Wei X, Decker JM, Liu H, Zhang Z, Arani RB, Kilby JM, et al. Emergence of resistant human immunodeficiency virus type 1 in patients receiving fusion inhibitor (T-20) monotherapy. Antimicrob Agents Chemother 2002;46:1896–905.

Weiner MP, Costa GL, Schoettlin W, Cline J, Mathur E, Bauer JC. Site-directed mutagenesis of double-stranded DNA by the polymerase chain reaction. Gene 1994;151:119–23.

Wild C, Oas T, McDanal C, Bolognesi D, Matthews T. A synthetic peptide inhibitor of human immunodeficiency virus replication: correlation between solution structure and viral inhibition. Proc Natl Acad Sci U S A 1992;89: 10537–41.

Xu L, Pozniak A, Wildfire A, Stanfield-Oakley SA, Mosier SM, Ratcliffe D, et al. Emergence and evolution of enfuvirtide resistance following long-term therapy involves heptad repeat 2 mutations within gp41. Antimicrob Agents Chemother 2005;49:1113–9.

Xu Y, Hixon MS, Dawson PE, Janda KD. Development of a FRET assay for monitoring of HIV gp41 core disruption. J Org Chem 2007;72:6700–7.

Supplemental Material can be found at:
http://www.jbc.org/content/suppl/2008/12/11/M807169200.DC1.html

THE JOURNAL OF BIOLOGICAL CHEMISTRY VOL. 284, NO. 8, pp. 4914–4920, February 20, 2009

Design of Peptide-based Inhibitors for Human Immunodeficiency Virus Type 1 Strains Resistant to T-20*[S]

Received for publication, September 16, 2008, and in revised form, December 3, 2008 Published, JBC Papers in Press, December 10, 2008, DOI 10.1074/jbc.M807169200

Kazuki Izumi[‡], Eiichi Kodama[‡1], Kazuya Shimura[‡], Yasuko Sakagami[‡], Kentaro Watanabe[§], Saori Ito[§], Tsuyoshi Watabe[§], Yukihiro Terakawa[§], Hiroki Nishikawa[§], Stefan G. Sarafianos[¶], Kazuo Kitaura[§], Shinya Oishi[§], Nobutaka Fujii[§], and Masao Matsuoka[‡]

From the [‡]Institute for Virus Research, Kyoto University, 53 Kawaramachi, Shogoin, Kyoto 606-8507, Japan, the [§]Graduate School of Pharmaceutical Sciences, Kyoto University, 46-29 Yoshida, Shimoadachi-cho, Kyoto 606-8501, Japan, and the [¶]Christopher S. Bond Life Sciences Center and Department of Molecular Microbiology and Immunology, University of Missouri School of Medicine, Columbia, Missouri 65211

Enfuvirtide (T-20) is a fusion inhibitor that suppresses replication of human immunodeficiency virus (HIV) variants with multi-drug resistance to reverse transcriptase and protease inhibitors. It is a peptide derived from the C-terminal heptad repeat (C-HR) of HIV-1 gp41, and it prevents interactions between the C-HR and the N-terminal HR (N-HR) of gp41, thus interfering with conformational changes that are required for viral fusion. However, prolonged therapies with T-20 result in the emergence of T-20-resistant strains that contain primary mutations such as N43D in the N-HR of gp41 (where T-20 and C-HR bind) that help the virus escape at a fitness cost. Such variants often go on to acquire a secondary mutation, S138A, in the C-HR of gp41 region that corresponds to the sequence of T-20. We demonstrate here that the role of S138A is to compensate for the impaired fusion kinetics of HIV-1s carrying primary mutations that abrogate binding of T-20. To preempt this escape strategy, we designed a modified T-20 variant containing the S138A substitution and showed that it is a potent inhibitor of both T-20-sensitive and T-20-resistant viruses. Circular dichroism analysis revealed that the S138A provided increased stability of the 6-helix bundle. We validated our approach on another fusion inhibitor, C34. In this case, we designed a variant of C34 with the secondary escape mutation N126K and showed that it can effectively inhibit replication of C34-resistant HIV-1. These results prove that it is possible to design improved peptide-based fusion inhibitors that are efficient against a major mechanism of drug resistance.

HIV-1[2] entry into the target cells is mediated by two envelope glycoproteins, gp120 and gp41, that form a trimeric gp120·gp41 complex. After binding of gp120 to the CD4 receptor and CCR5 (or CXCR4) coreceptor on the surface of the target cell, the gp41 trimer forms an extended conformation of the three helices that allows a hydrophobic fusion peptide to be inserted into the target cell membrane, generating an intermediate that is anchored to both cellular and viral membranes. After this step, the gp41 is believed to start refolding to a more stable 6-helix bundle composed of the α-helical trimer of the N-terminal heptad repeat (N-HR) folded into an anti-parallel conformation with the three C-terminal heptad repeats (C-HR) (1, 2). This refolding brings the viral and cellular membranes together to catalyze fusion.

The transition of the extended intermediate to the 6-helix bundle can be inhibited by the addition of exogenous peptides derived from gp41 C-HR (Fig. 1*A*) that prevent the formation of the 6-helix bundle and inhibit the HIV-1 fusion with the target cells (3–6). T-20, a 36-amino acid peptide derived from C-HR, effectively suppresses *in vivo* replication of HIV-1 resistant to inhibitors of reverse transcriptase and protease (7, 8). However, HIV-1 variants resistant to T-20 have recently emerged carrying primary mutations in the Leu-33–Leu-45 region of the N-HR domain (9–15). Among them, V38A and N43D seem to be major primary mutations for T-20 resistance. Meanwhile, a secondary mutation at the C-HR region (S138A) has been reported to enhance T-20 resistance with an as yet undefined mechanism (9, 14, 15) (Fig. 1*B*).

The mechanism of resistance to C34, another C-HR peptide-based inhibitor of HIV fusion, has been the subject of multiple studies (13, 16). Because of a 22-amino acid overlap between the T-20 and C34 peptides (Fig. 1*B*), HIV-1 has developed primary mutations for C34 resistance *in vitro* at the identical Leu-33–Leu-45 region of the peptides. During *in vitro* selection of C34 resistance, we identified a mutation in the C-HR domain, N126K, that is also observed in some T-20-resistant clinical variants (10, 15, 17). We showed that N126K conferred resistance to C34 by compensating for the impaired intra-gp41 inter-

* This work was supported, in part, by National Institutes of Health Grants AI076119, AI079801, and AI074389 (to S. G. S.). This work was also supported in part by grants from the Ministry of Health and Welfare and the Ministry of Education, Culture, Sports, Science, and Technology of Japan (to E. K., S. O., and N. F.), the Japan Health Sciences Foundation (to E. K., S. O., N. F., and M. M.), the 21st Century COE program (to K. I., S. I., and H. N.), and a Japan Society for the Promotion of Science research fellowship (to H. N.). The costs of publication of this article were defrayed in part by the payment of page charges. This article must therefore be hereby marked "*advertisement*" in accordance with 18 U.S.C. Section 1734 solely to indicate this fact.

[S] The on-line version of this article (available at http://www.jbc.org) contains supplemental Figs. 1 and 2 and Tables 1 and 2.

[1] To whom correspondence should be addressed. Tel. and Fax: 81-75-751-3986; E-mail: ekodama@virus.kyoto-u.ac.jp.

[2] The abbreviations used are: HIV, human immunodeficiency virus; T-20, enfuvirtide; HR, heptad repeat; MAGI, multinuclear activation of galactosidase indicator; EC_{50}, 50% effective concentration; T_m, melting temperature; CD, circular dichroism; shRNA, short hairpin RNA; WT, wild-type.

Supplemental Material can be found at:
http://www.jbc.org/content/suppl/2008/12/11/M807169200.DC1.html

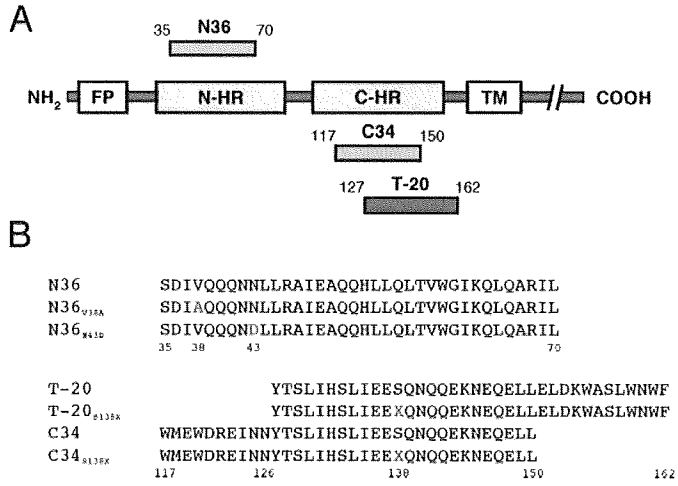

FIGURE 1. **Schematic view of gp41 and peptide sequence.** *A*, structure of HIV-1 gp41 and locations of N-HR or C-HR peptides (*FP*, fusion peptide; *TM*, transmembrane domain). *B*, amino acid sequences of peptides used in this study. Only the amino acid located at Ser-138 was substituted with all physiological amino acids (*X*), as Asn-126 lies outside of the amino acid sequence of T-20.

action by a primary mutation, I37K (13). N126K was initially identified in background of V38A, another primary mutation, for T-20 resistance *in vivo* (17). Baldwin *et al.* (17, 18) demonstrated a striking T-20-dependent replication phenotype in the V38A/N126K variant and proposed that T-20 acts as a safety pin to prevent premature formation of helical bundle, as N126K enhanced binding capacity of the introduced C-HR to N36 with V38A. Taken together, these studies suggest that mutations in the C-HR serve as secondary mutations.

In this study we show that the main role of secondary mutations that follow the appearance of primary mutations during treatment with peptide-based fusion inhibitors is to compensate for the impairment in replication kinetics that is caused by the primary mutations (supplemental Fig. 1). Based on this finding we hypothesized that analogs of T-20 carrying substitutions corresponding to secondary T-20 resistance mutations should be active against both wild-type and T-20-resistant viruses containing primary mutations. Indeed, our results confirmed our hypothesis and showed that T-20 with the S138A substitution ($T\text{-}20_{S138A}$) has a strong anti-HIV-1 activity even against T-20-resistant clones. Moreover, we demonstrate that this restoration is concomitant to improved binding of $C\text{-}HR_{S138A}$ to $N\text{-}HR_{N43D}$, suggesting that our approach utilizing the resistance-associated mutations to design peptides may provide useful broad insights into effective peptide-based therapies.

EXPERIMENTAL PROCEDURES

Cells and Viruses—MT-2 cells were grown in RPMI 1640 medium. 293T cells were grown in Dulbecco's modified Eagle's medium-based culture medium. HeLa-CD4-LTR-β-gal cells were kindly provided by M. Emerman through the AIDS Research and Reference Reagent Program, Division of AIDS, NIAID, National Institutes of Health (Bethesda, MD) and were used for the drug susceptibility assay as described previously (13, 19, 20). An HIV-1 infectious clone, pNL4–3 (21), was used for generation of HIV-1 variants.

Antiviral Agents—The peptides used in this study were synthesized as described previously (6).

Determination of Drug Susceptibility of HIV-1—The peptide sensitivity of infectious clones was determined by the multinuclear activation of galactosidase indicator (MAGI) assay as described previously (13). Briefly, the target cells (HeLa-CD4-LTR-β-gal; 10^4 cells/well) were plated in 96-well flat microtiter culture plates. On the following day the cells were inoculated with the HIV-1 clones (60 MAGI unit/well, giving 60 blue cells after 48 h of incubation) and cultured in the presence of various concentrations of drugs in fresh medium. Forty-eight hours after viral exposure, all the blue cells stained with 5-bromo-4-chloro-3-indolyl-β-D-galactopyranoside (X-gal) were counted in each well. The activity of test compounds was determined as the concentration that blocked HIV-1 replication by 50% (50% effective concentration, (EC_{50}).

Generation of Recombinant HIV-1 Clones—Recombinant infectious HIV-1 clones, carrying various mutations, were generated as described previously (13). Each molecular clone was transfected into 293T cells with *Trans*IT® (Madison, WI). After 48 h, the supernatants were harvested and stored at −80 °C until use.

Circular Dichroism Spectroscopy—Each peptide (10 μM) was mixed with 10 mM phosphate-buffered saline, pH 7.4, and the data were collected using a Jasco spectrometer (Model J-710; Jasco, Tokyo, Japan) equipped with a thermoelectric temperature controller. The thermal stability was assessed by monitoring the change in the circular dichroism signal at 222 nm. The midpoint of the thermal unfolding transition (melting temperature, (T_m) of each complex was determined as described previously (6).

Viral Replication Kinetics Assay—MT-2 cells (10^5 cells/3 ml) were infected with each virus preparation (1000 MAGI unit) for 16 h. The infected cells were then washed and cultured in a final volume of 3 ml. The culture supernatants were harvested after infection on days 2–7, and the levels of p24 antigen were determined (22).

For each competitive HIV-1 replication assay, two infectious clones of interest that had been previously titrated were mixed and added to MT-2 cells (10^5 cells/3 ml) as described previously (13, 22) with minor modifications. To ensure that the two infectious clones being compared were of approximately equal infectivity, a fixed amount (500 MAGI unit) of one infectious clone was mixed with three different amounts (250, 500, and 1000 MAGI unit) of the other infectious clone. On day 1, one-third of the infected MT-2 cells were harvested and washed twice with phosphate-buffered saline, and the cellular DNA was extracted. The purified DNA was subjected to nested PCR and then direct DNA sequencing. The HIV-1 co-culture, which best approximated a 50:50 mixture on day 1, was further propagated. Every 3–4 days, the co-culture supernatant (100 μl) was transmitted to new uninfected MT-2 cells (5×10^5 cells/3 ml). The cells harvested at the end of each passage were subjected to direct sequencing, and the viral population change was determined.

Structure Modeling of gp41 S138A Mutant Core—The gp41 core model was built using the coordinates of crystal structure of the N36/C34 complex (23) (PDB code 1AIK). The coordi-

Supplemental Material can be found at:
http://www.jbc.org/content/suppl/2008/12/11/M807169200.DC1.html

Application of Resistant Mutations to Enfuvirtide

TABLE 1

Antiviral activity of T-20-derived peptides against T-20-resistant gp41 recombinant viruses

Anti-HIV activity was determined with the MAGI assay. The data shown are the mean values and S.D. that were obtained from the results of at least three independent experiments. Shown in parentheses are the -fold increases in resistance (increase in EC_{50} value) calculated by comparison to a reference virus. Increases of >10-fold are indicated in bold.

	EC_{50}			
	HIV-1_{WT}[a]	HIV-1_{V38A}	HIV-1_{N43D}	HIV-$1_{N43D/S138A}$
	nM			
T-20	2.4 ± 0.6	23 ± 8.2 (9.6)	49 ± 10 (20)	84 ± 16 (35)
Small				
T-20_{S138G}	1.3 ± 0.5 (0.5)	65 ± 8.8 (27)	141 ± 26 (59)	185 ± 68 (77)
T-20_{S138A}	0.6 ± 0.1 (0.3)	3.6 ± 1.7 (1.5)	3.5 ± 0.9 (1.5)	3.2 ± 1.0 (1.3)
Hydrophobic				
T-20_{S138V}	0.4 ± 0.2 (0.2)	31 ± 14 (13)	22 ± 3.5 (9.2)	23 ± 5.7 (9.6)
T-20_{S138L}	0.7 ± 0.1 (0.3)	13 ± 6 (5.4)	2.9 ± 0.7 (1.2)	2.2 ± 0.4 (0.9)
T-20_{S138I}	0.5 ± 0.1 (0.2)	4.9 ± 2 (2)	2.9 ± 0.8 (1.2)	2.4 ± 0.6 (1)
T-20_{S138M}	0.7 ± 0.2 (0.3)	4.4 ± 0.1 (1.8)	1.7 ± 0.5 (0.7)	1.2 ± 0.4 (0.5)
T-20_{S138P}	446 ± 167 (186)	>1000 (>416)	>1000 (>416)	>1000 (>416)
Nucleophilic				
T-20_{S138T}	0.9 ± 0.2 (0.4)	39 ± 8.5 (16)	161 ± 35 (67)	124 ± 43 (52)
Aromatic				
T-20_{S138F}	9.4 ± 2.6 (4)	203 ± 89 (85)	393 ± 119 (164)	478 ± 116 (200)
T-20_{S138Y}	25 ± 9 (10)	516 ± 223 (215)	>1000 (>416)	>1000 (>416)
T-20_{S138W}	29 ± 14 (12)	>1000 (>416)	>1000 (>416)	>1000 (>416)
Amide				
T-20_{S138N}	19 ± 4 (8)	>1000 (>416)	>1000 (>416)	>1000 (>416)
T-20_{S138Q}	34 ± 11 (14)	>1000 (>416)	>1000 (>416)	>1000 (>416)
Acidic				
T-20_{S138D}	210 ± 94 (88)	>1000 (>416)	>1000 (>416)	>1000 (>416)
T-20_{S138E}	283 ± 80 (118)	>1000 (>416)	>1000 (>416)	>1000 (>416)
Basic				
T-20_{S138H}	210 ± 85 (88)	>1000 (>416)	>1000 (>416)	>1000 (>416)
T-20_{S138K}	708 ± 145 (295)	>1000 (>416)	>1000 (>416)	>1000 (>416)
T-20_{S138R}	362 ± 114 (150)	>1000 (>416)	>1000 (>416)	>1000 (>416)

[a] To improve the replication kinetics, D36G mutation, observed in the majority of HIV-1 strains, was introduced into the NL4-3 background used in this study (reference virus).

nates of the water molecules were removed. Additionally, the hydrogen atoms were placed in optimal positions and refined by the energy minimization with the AMBER9 program (24) using the FF99 force field. Ser-138 in the gp41 core model was replaced with alanine (replacement of -OH with -H), and the positions of the hydrogen atoms were refined as described above. The S138A mutant core model (N36/$C34_{S138A}$ complex) was further optimized by the energy minimization using the FF99 force field with the restraints on each of the three residues of N and C termini and the backbone atoms. The restraint weight was 5.0 kcal/mol Å^2.

RESULTS

Effect of Amino Acid Substitutions at 138 on Antiviral Activities—We chemically synthesized peptide analogs of T-20 with all natural amino acid substitutions at the 138 position (T-20_{S138X}) and evaluated them for their ability to inhibit three major T-20-resistant clones using the MAGI assay (13) (Table 1). The results indicated that only T-20_{S138A} inhibited replication of T-20-resistant clones as efficiently as the wild-type clone. Substitution to glycine enhanced T-20 activity, but unlike T-20_{S138A}, T-20_{S138G} reduced its activity against T-20-resistant clones by ~2–3-fold as compared with the parental peptide, T-20. Substitutions to hydrophobic amino acids leucine, isoleucine, and methionine maintained their anti-HIV-1 activity; however, those to valine reduced anti-HIV-1 activity to T-20-resistant clones. The proline substitution drastically decreased the anti-HIV-1 activity of the peptide inhibitors.

Nucleophilic amino acid at position 138 of T-20 (T-20_{S138T}) showed similar profiles. Conversely, aromatic and amide substitutions reduced the anti-HIV-1 activity of T-20 against HIV-1_{WT}- and T-20-resistant clones. Other amino acid substitutions, especially acidic and basic amino acids, decreased the anti-HIV-1 inhibitory activity even against HIV-1_{WT}. These results suggest that smaller hydrophobic (Ala > Leu, Ile) or more flexible (Met > Thr) residues are preferred in this position. Furthermore, the α-helical structure is important for the interaction, as a mutation to proline which is expected to disrupt the helix (25) resulted in an inactive T-20 analog.

Circular Dichroism—To clarify the mechanism by which the substitutions at Ser-138 influence the antiviral activity of T-20 derivatives, we examined the binding affinities of these peptides to N-HR using circular dichroism (CD) analysis (Fig. 2). CD spectra reveal the presence of stable α-helical structure of the 6-helix bundle that is a requisite for biological activity and is thought to be mechanistically and thermodynamically correlated with HIV-1 fusion (26). Therefore, CD spectra typically at 222 nm indicate interaction of N-HR (N36) and C-HR (T-20 or C34). Because T-20 does not interact significantly *in vitro* with the N36 peptide, which is derived from amino acids 35–70 of N-HR, we used a derivative of C34, a peptide that overlaps with T-20 and also inhibits HIV fusion by the same mechanism. The C34 derivative contained the analogous T-20 substitutions described above (Fig. 1*B*). Consistent with antiviral activities, a mixture of N36 and $C34_{S138P}$ or $C34_{S138W}$ showed no apparent or reduced α-helicity, respectively. For binding with $N36_{V38A}$

Supplemental Material can be found at:
http://www.jbc.org/content/suppl/2008/12/11/M807169200.DC1.html

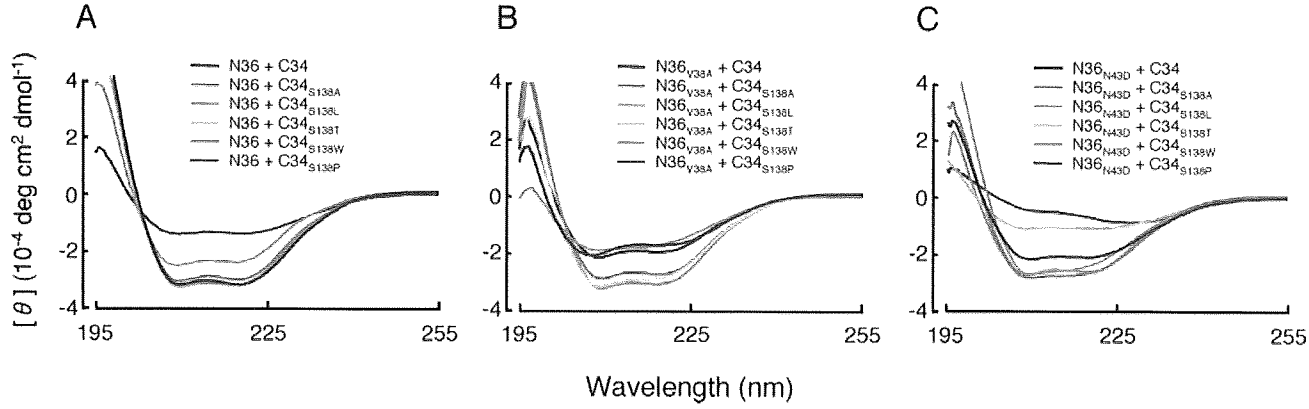

FIGURE 2. **CD spectra of $C34_{S138X}$ complexes with N36 (*A*), $N36_{V38A}$ (*B*), and $N36_{N43D}$ (*C*) are shown.** Equimolar amounts (10 μM) of the N- and C-HR peptides were incubated at 37 °C for 30 min in phosphate-buffered saline. The CD spectra of each mixture were then collected at 25 °C using a Jasco (Model J-710) spectropolarimeter.

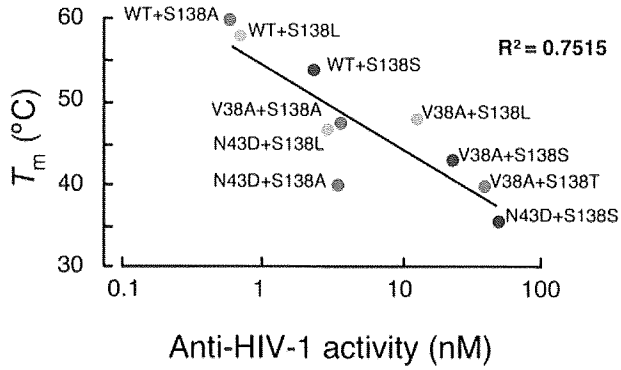

FIGURE 3. **Correlation of T_m values of complexes formed from N36 and C34 peptides (Fig. 2) and anti-HIV-1 activities of T-20_{S138X} (Table 1).**

or $N36_{N43D}$, sufficient α-helicity at 25 °C was observed only in $C34_{S138A}$, $C34_{S138L}$, and $C34_{S138T}$ or $C34_{S138A}$, $C34_{S138L}$, and $C34_{S138W}$, respectively (Fig. 2, *A–C*).

To determine the thermal stability of the helical complexes formed from the N36 and C34 peptides, we measured the melting temperature (T_m) of each complex (supplemental Table 1). The sigmoidal transition of the CD signal at 222 nm correlates with the thermal stability of the helical complexes formed from the N36 and C34 peptides, which in turn are indicative of the binding affinity of these peptides. The melting temperature (T_m) indicating the 50% disruption of 6-helix bundle was comparatively evaluated. Complexes of N36 and C34 containing the S138A or S138L substitutions (N36/$C34_{S138A}$ or N36/$C34_{S138L}$) showed high thermal stability, comparable with that of the wild-type N36/C34 complex. Similarly, the addition of the S138A or S138L also improved the thermal stability of the $N36_{N43D}$/C34 complex. These results reveal a striking correlation between the thermal stability and the anti-HIV-1 activity of the complexes (R^2 = 0.75, Fig. 3). The low T_m value of the complex formed from $N36_{N43D}$ and C34 suggests that virus containing the N43D mutation shows high resistance to T-20, likely due to less favorable thermodynamics that are expected to drive the formation of the 6-helix bundles containing T-20 inhibitor.

Antiviral Activity of Substituted C34 at Ser-138—To confirm that binding of C34 to N-HR is indeed representative of T-20 binding to N-HR, we examined the anti-HIV-1 activities of

TABLE 2

Antiviral activity of $C34_{N126K}$ peptides against C34-resistant gp41 recombinant viruses

Anti-HIV activity was determined by the MAGI assay. The data shown are the mean values and S.D. that were obtained from the results of at least three independent experiments. Shown in parentheses are the -fold increases in resistance (increase in EC_{50} value) calculated by comparison to a reference virus. The increase of >10-fold is indicated in bold.

	EC_{50}	
	HIV-1_{WT} [a]	HIV-$1_{\Delta V4/I37K/N126K/L204I}$ [b]
	HM	
C34	1.6 ± 0.35	114 ± 29 (71)
$C34_{N126K}$	0.95 ± 0.22 (0.6)	1.1 ± 0.5 (0.7)

[a] To improve the replication kinetics, the D36G mutation, observed in majority of HIV-1 strains, was introduced into the NL4-3 background used in this study (reference virus).

[b] C34-resistant HIV-1 was constructed with the reference virus as described (13). ΔV4 indicates 5 amino acids deletion (FNSTW) in the V4 region of gp120.

C34-derived peptides that have S138A substitutions. The $C34_{S138A}$ and $C34_{S138L}$ peptides showed potent anti-HIV-1 activities, similar to T-20_{S138A} and T-20_{S138L} (supplemental Table 2). Based on these findings, we conclude that the stability of complexes comprised of modified C34s and N36s containing T-20 resistance mutations offers a good measure of the binding affinity of T-20_{S138X} to N-HR.

Antiviral Activity of C34 with N126K—We have recently identified another mutation at the N-HR of gp41 (N126K) during exposure of HIV-1 to C34 *in vitro* (13). The N126K has been occasionally observed after prolonged T-20-containing therapy (10, 15). Here we have confirmed that the $C34_{N126K}$ peptide can also suppress a C34-resistant clone containing several mutations: I37K/N126K/L204I (Table 2). Therefore, peptides designed to have compensatory mutations seem to have potent antiviral activity. However, because residue 126 is located outside the amino acid sequence of T-20 (Fig. 1*B*), we could not examine the effect of N126K substitution on T-20 activity.

Replication Kinetics of Ser-138-substituted HIV-1—To evaluate the effect of Ser-138 substitutions on viral replication, we constructed molecular clones introducing several Ser-138 and determined their replication kinetics by measuring p24 gag antigen production in the culture supernatant. Single nucleotide changes to the TCA codon for Ser-138 may generate 4 amino acid substitutions, Ala, Thr, Leu, Pro, and Trp. As expected, the compensative substitution, S138A, in the T-20

Supplemental Material can be found at:
http://www.jbc.org/content/suppl/2008/12/11/M807169200.DC1.html

resistance mutation N43D background enhanced replication kinetics of the N43D-containing clone as shown in supplemental Fig. 1. However, in the WT background the S138A appeared to decrease production of p24 as compared with HIV-1_{WT} (Fig. 4). Other substitutions also reduced their replication kinetics. Interestingly, the S138W substitution did not show measurable p24 production. Syncytia induction and single cycle replication kinetics of the Ser-138-substituted HIV-1 were also examined (supplemental Fig. 2). Sizes of syncytia of each virus formed in the MAGI cells (supplemental Fig. 2, *panels A–E*) were associated with p24-normalized single-cycle infectivities (supplemental Fig. 2, *panel F*) and multicycle replication kinetics (Fig. 4). These results suggest that substitutions at Ser-138 are not likely to appear in the absence of T-20 therapy or the emergence of N43D mutation.

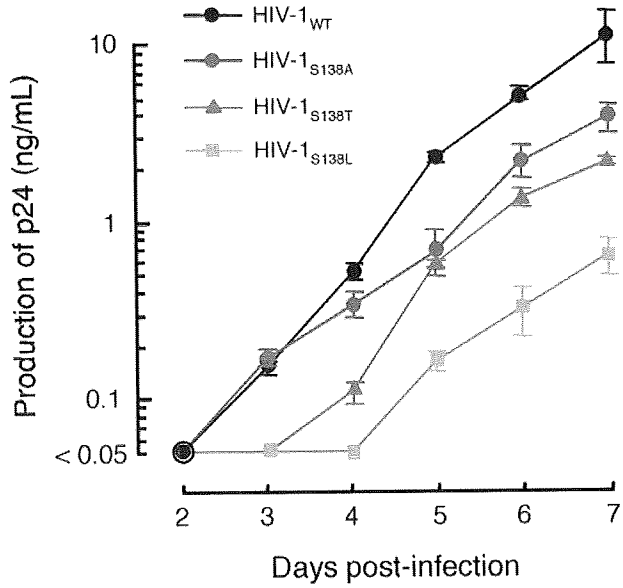

FIGURE 4. **Replication kinetics of HIV-1_{S138X} variants (*X*, any natural amino acid).** HIV-1_{S138A} (*bright red circles*) showed replication kinetics comparable with those seen for HIV-1_{WT} (*blue circles*). Replication of HIV-1_{S138T} (*emerald green triangles*) was reduced, somewhat surprisingly, as both threonine and serine are β-hydroxy amino acids, albeit with different hydrophobicity and torsional flexibility. HIV-1_{S138L} (*orange squares*) also showed reduced replication kinetics. Note that HIV-1_{S138P} and HIV-1_{S138W} failed to replicate (data not shown). Results shown are representative of three independent experiments. An identical order of replication kinetics was observed. Productions of p24 antigen on days 4–7 between HIV-1_{WT} and HIV-1_{S138A} were significant (*t* test, $p < 0.05$).

Structure Modeling—The side chain of amino acid 138 (Ser or Ala) closely contacts with the hydrophobic pocket formed by Leu-44 and Leu-45 in the N-HR. The mutation from Ser to Ala increases hydrophobicity and may help to stabilize the N-HR/C-HR complex related with the potency of the HIV-1 fusion inhibitors (Fig. 5). Larger hydrophobic substitutions such as S138W, S138L, or S138I are likely to sterically interfere with efficient packing of the N-HR and C-HR helices. Similarly, introduction of charged residues at this region of the interface would also disrupt the hydrophobic environment and result in destabilized helix bundles, consistent with the biochemical and virological findings (Figs. 2–4 and Table 1).

Based on crystallographic studies (27, 28), we observe that the T-20 resistance N43D mutation should affect interactions between helices in the 6-helix bundle. Specifically, residue 46 of N-HR is proximal to residue Glu-137 of the C-HR helix of another molecule in the 6-helix bundle. We believe that this increase in proximal negative charges and juxtaposition of Asp-36 next to Glu-137 may destabilize the formation of the 6-helix bundle in a way that results in reduced efficiency of fusion and reduced replication kinetics. Increase of the hydrophobic interactions by introduction of the S138A mutation should help overcome the negative effects of the N43D mutation.

DISCUSSION

In this study we demonstrate that by introducing a secondary resistance mutation into the sequence of peptide-fusion inhibitors such as C34 and T-20, we can suppress efficiently replication of wild-type and of fusion inhibitor-resistant HIV-1. Our circular dichroism analysis revealed that C-HR-based fusion inhibitors that carry secondary resistance mutations can form tight 6-helix bundles with N-HR that contains primary resistance mutations responsible for T-20 resistance. A similar approach has been applied for the development of short hairpin RNA (shRNA) sequences that inhibit HIV-1 replication (29). The synthesized shRNA with mutations that confers resistance to the parental shRNA effectively suppressed replications of shRNA resistant HIV-1 but not wild-type HIV-1. Therefore, it is possible to gain valuable insights from the resistance information and directly apply it to design new peptides or oligonucleotides in the case of shRNA that preempt the viral escape mechanism and suppress resistant variants. Moreover, this strategy should not result in more adverse effect than those that might be obtained during use of the original peptide or oligonucleotide reagents.

Recently we (6, 30, 31) and others (5) reported that hydrophilic amino

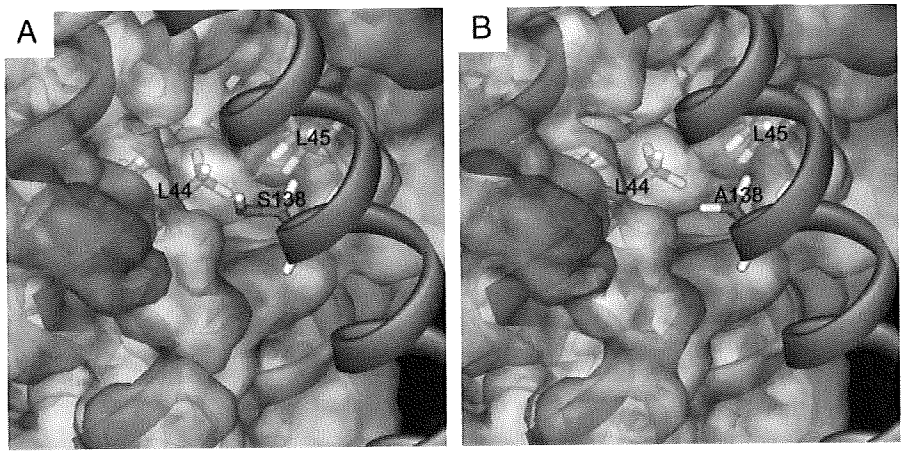

FIGURE 5. **Structure of gp41 at the region near position 138 in the C-HR.** *A*, crystal structure of the N36/C34 complex (PDB code 1AIK). *B*, computational structure modeling of the S138A mutant (N36/$C34_{S138A}$ complex). N-HR and C-HR helices are colored *green* and *orange*, respectively. The van der Waals surface of only N-HR is shown and colored according to the electrostatic potential.